β-catenin do not localize with WNT destruction complex components in tankyrase inhibitor resistant HCT-15 colorectal cancer cells

Maria Melheim
Mastergrad i Bioteknologi, retning molekylærbiologi

Table of contents

Acknowledgements

Abstrakt

Blant kaskader og signalveier i cellene har feil i WNT signalveien vist å ha stor betydning i kreftutvikling. I friske celler bytter signalveien på å være aktiv og inaktiv og regulerer på denne måten ulike systemer i cellene. Når mutasjoner oppstår medfører dette uttrykk av konstant aktiv WNT signalering. Tankyrase har vist seg å være et WNT signalaktiveringsprotein, og fungerer ved å markere AXIN1/2 for degradering. Ved å hemme tankyrase vil AXIN1/2 blir stabilisert og β-catenin proteinnivå vil synke med en følgende reduksjon av proliferasjon.

Tarmkreft cellelinjen COLO 320DM har vist seg å være sensitiv mot tankyrase hemming hvor β-catenin blir merket for degradering av destruksjonskomplekset, men ikke alle tarmkreft cellelinjer er sensitive mot tankyrase hemming. Et eksempel på en resistent tarmkreft cellelinje er HCT-15. Målet med denne oppgaven er derfor å undersøke om β-catenin er lokalisert med WNT destruksjonskomplekskomponentene i HCT-15 celler, eller om separerte grupper av WNT destruksjonskomleks-komponenter holder β-catenin vekk fra komplekset, som av den grunn unngår å bli degradert.

Analyser bekreftet kolokalisering mellom TNKS1/2, GSK3β og AXIN2 i cytoplasmamembranen i HCT-15 celler behandlet med tankyrase hemmende behandling, men β-catenin var ikke i disse kompleksene. Med MEK hemmende behandling ble både β-catenin og TNKS-kompleksene frigjort fra cytoplasmamembranen, og det ble observert sterk reduksjon i proliferasjonsraten. Likevel ble ikke β-catenin observert i TNKS-kompleksene, i tillegg til at protein nivået av β-catenin var upåvirket. Dette beviste at det er β-catenin uavhengig proliferasjon i HCT-15 celler, som igjen ble bekreftet ved esiRNA mediert fjerning av β-catenin. Hvilke mekanismer som kontrollerer proliferasjonen i HCT-15 celler er ikke fullstendig forstått, men resultatene i denne oppgaven gir en indikasjon på at EGFR signalveien og AXIN1/2 er involvert.

Abstract

Among the cascades and signaling pathways inside the cells, defects found in the WNT/β-catenin signaling pathway play a significant role in human cancer. The WNT/β-catenin signaling pathway switches between an "on" and "off" state, however in cancer, mutations creates a constitutive active signaling. Over the last years researchers have drawn attention towards a poly-ADP ribose polymerase called tankyrase, which are found to activate the WNT/β-catenin signaling pathway through degradation of AXIN1/2 proteins. By inhibiting tankyrase, stabilization of AXIN1/2 decreases β-catenin protein levels with subsequent reduction in proliferation of many colorectal cancer cell lines.

The COLO 320DM colorectal cancer cell line has shown to be sensitive to tankyrase inhibition (TNKSi), where β-catenin is subsequently targeted for degradation by the destruction complex. However, there are several colorectal cancer cell lines that are insensitive to TNKSi, where neither β-catenin nor proliferation is affected. The HCT-15 colorectal cancer cell line is one such TNKSi resistant cell line. The aim of this thesis was therefore to investigate whether β-catenin is localized with WNT destruction complex components in HCT-15 cells, or whether separate pools of destruction complex components protect β-catenin from degradation.

Analysis confirmed co-localization between TNKS1/2, GSK3β and AXIN2 in the cytoplasmic membrane upon TNKSi in HCT-15 cells. However, β-catenin was not under any tested condition co-localized with the destruction complex. Upon inhibition of MEK, a release of both TNKS1/2 containing complexes and β-catenin from the cell membrane occurred, with subsequent strong reduction in proliferation rate. However, β-catenin did not co-localize with the TNKS1/2 containing complexes. β-catenin protein levels were not affected by the MEKi, confirming a β-catenin independent proliferation, which was also confirmed by knock down of β-catenin. Which mechanisms controlling proliferation rate of HCT-15 cells are not fully understood, however results indicate that the EGFR-pathway and AXIN1/2 are involved.

1. Introduction

Every year the Norwegian Institute of Public Health publishes the annual mortality statistics [1]. Nationally, cardiovascular disease has been the most frequent cause of death in Norway, but cancer is currently about to pass heart disease on the list. In 2015 in excess of 40,000 died in Norway, where 27,2 % of these was caused by cancer [1], and the Norwegian Institute of Public Health claim that about 40 % will get cancer during their lifetime [2]. The Norwegian cancer registry have registered the most frequently occurring cancers for 2015, as prostate cancer, breast cancer, lung cancer, colon cancer and melanoma [3]. Nationally, colorectal cancer (CRC) is the second most common cancer, when simultaneously looking at both sexes, with about 4,100 new cases in 2015 [4].

Cancer

A fundamental feature of cancer is the progression of abnormal proliferation from one single cell, as a result of genetic alterations, which results in tumor development [5]. This uncontrolled growth is caused by an accumulation of different abnormalities affecting regulatory mechanisms in the cells, such as mechanisms that regulate survival, differentiation and proliferation. This uncontrolled proliferation leads to a population of clonally derived cells, which together forms the tumor. Additional mutations further occur within the tumor population, inducing more rapid growth.

A tumor can be both benign and malignant, where only malignant tumors are referred to as cancers [5]. A benign tumor is constricted to one location, with no possibility to neither invade surrounding tissue nor spread to different body sites. In contrast, a malignant tumor will invade the surrounding tissue and will via the circulatory or lymphatic system spread throughout the body

Colorectal cancer

CRC is defined as cancerous growth in the appendix, colon, and rectum, and is the second leading cause of cancer-related death in the Western world [6]. About 75 % of patients get the sporadic form of CRC, whereas the remaining 25 % are suggested to have a genetic predisposing, with common exposures among family members. Patients with the sporadic colorectal carcinomas are neither familial nor inherited predisposed, but illness is likely a result of normal aging, environmental and dietary factors. Symptoms typical for colorectal cancer are changes in bowel habits, fecal occult blood and abdominal pain, among others [7]. In most cases there is no defined cause of disease, although physical inactivity, overweight and high consumption of alcohol and tobacco are factors which may increase the risk. In addition, age, inheritance and genetics (such as ulcerative colitis and Crohn`s disease) may also play a role. A well known example is familial adenomatous polyposis (FAP), which gives a higher risk to develop colorectal cancer[8]. The FAP syndrome is a dominantly inherited, autosomal disorder developed due to germline mutations in the *adenomatous polyposis coli APC* tumor-suppressor gene [9]. Upon FAP syndrome, development of adenomatous polyps occur in over 90 % of patiens by age 35 years, which occurs to be the precursor for most CRC and the risk of cancer development is nearly 100 % [8, 9].

Interestingly, the incidence rate of CRC is extremely varied between different geographical areas [10]. In Africa, Asia and parts of Latin America the incidence rate of CRC is relatively low, while in Northern Europe, U.S, New Zealand and Australia; which also are termed as the "Western countries", the incidence rate is extremely high. In addition, when populations from low-risk countries immigrate to high-risk countries they acquire an increased cancer risk [11]. This phenomenon underpins the possibility that environmental exposure influence the colorectal cancer probability, maybe through higher consumptions of red meat and a higher quantity of dietary fat.

Mutations in a number of tumor suppressor genes and DNA mismatch repair genes are observed as common denominators in the development of colorectal cancer [6]. A stepwise model of colorectal tumorigenesis from 1990 (figure 1) suggests that mutations in the *APC* gene induces an increased proliferation of colon epithelial cells

and thus give rise to a small neoplasm (such as an adenoma or polyp) [5, 8]. The small neoplasm obtains further increased size, induced by a second mutation emerging in the oncogenic *KRAS* gene, leading to the development of benign adenomas stage [5, 8]. Further mutations in *TP53* occur, which leads to malignancy. The malignant carcinomas will invade the benign adenoma tumor, through the basal lamina, and into underlying connective tissue, creating metastatic cancer stage [5, 8]. After invading throughout the connective tissue of the colon, the cancer cells will penetrate the colon wall and further invade other organs like the bladder or small intestine [5]. In addition, the cancer cells can enter the blood and lymphatic vessels, with subsequent metastasize throughout the body [5].
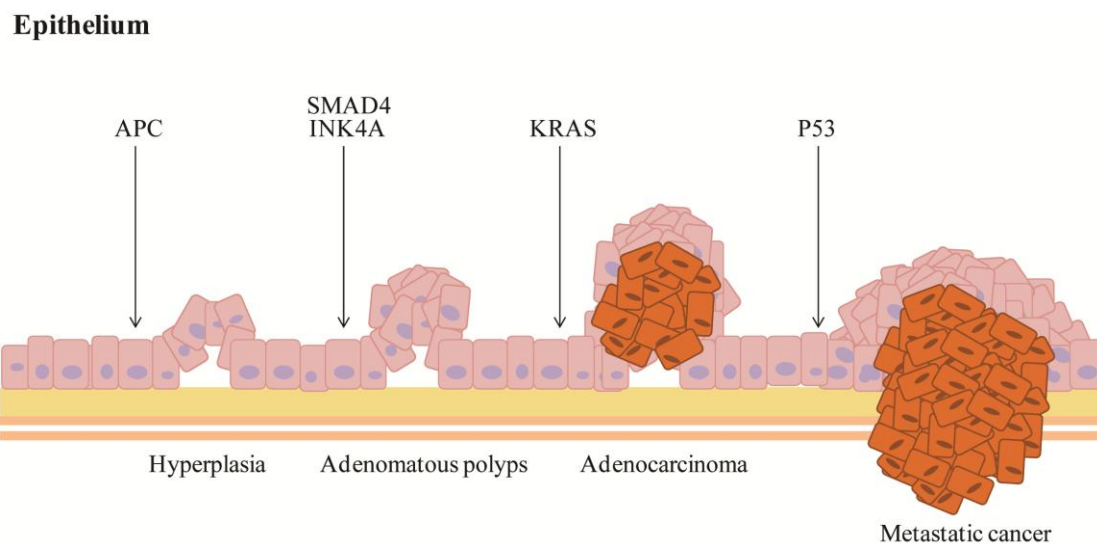
Figure 1. Epithelium cells with stages from normal growth to metastatic cancer.
A schematic drawing of the epithelium cell wall from normal cell layer obtaining different mutations leading to development of metastatic cancer.

Among the cascades and signaling pathways inside the cells, defects found in the WNT/β-catenin signaling pathway seem to play a significant role in human cancer [12], and have in the recent years received attention from cancer researchers because of the components` important role in tumor formation [13]. In fact, >80% of all colorectal cancers, both inherited and sporadic cases, are thought to be initiated by mutations in the *APC* gene. This directly links *APC* mutations to the early onset of colorectal cancer [14]. The *APC* tumor suppressor gene has an important role in

intercellular adhesion, cell cycle regulation, cytoskeleton stabilization and apoptosis [15]. In addition, *APC* has a tumor suppressing function by its capacity to down regulate β-catenin levels [16]. The gene encodes for the 300 kDa APC protein, which functions both as a functional scaffold in the WNT/β-catenin destruction complex, and is also responsible for promoting the ubiquitin-dependent proteasomal degradation of β-catenin in the WNT/β-catenin signaling pathway. More than 90% of APC mutations creates a premature stop codon, leading to a predominant truncation of the protein which mainly occur in the mutation cluster region (around aa1282-1582), with subsequent lack of several or all seven 20-amino-acid repeats (20-AARs) [8, 14]. The truncation display altered function by reducing APC`s ability to arrange correct chromosome segregation, as well as associating with microtubules or promote β-catenin binding and degradation [15].

Mutations in the *KRAS* gene is found in approximately 50% of all colorectal tumors, and accounts as the most somatic cancer-associated mutation prevalent in lung, pancreatic, biliary tract, colorectal, endometrial and cervical cancers [8, 17]. *KRAS* is one of three highly homologous *RAS* oncogenes (*KRAS, HRAS* and *NRAS*), which are induced by point mutations in codon 12, 13 or 61 in the *RAS* gene. These point mutations converts the *RAS* gene into an active oncogene that may further mutate in to several types of sporadic human cancers [18] [19]. RAS proteins are small GTPases which switch between inactive guanosine diphosphate (GDP)-bound and active guanosine triphosphate (GTP)-bound conformations in the EGFR-RAS-MAPK pathway [17]. The EGFR-RAS-MAPK pathway (figure 2) is activated by ligand binding to the epidermal growth factor receptor (EGFR), with subsequent recruitment of GRB2 and the guanine exchange factor, Son of sevenless (SOS). SOS further activates the GTPase protein RAS85D, with leading activation of the MAPK cascade. Active RAS first activate RAF, which in turn activates MAPK-extracellular signal-regulated kinase family protein (MEK1/2) by phosphorylation [20]. Activated MEK1/2 further activates a mitogen-activated protein kinase (MAPK) which is also known as the extracellular signal-regulated kinases (ERKs), which when activated are able to enter the nucleus and influence the target gene expression.
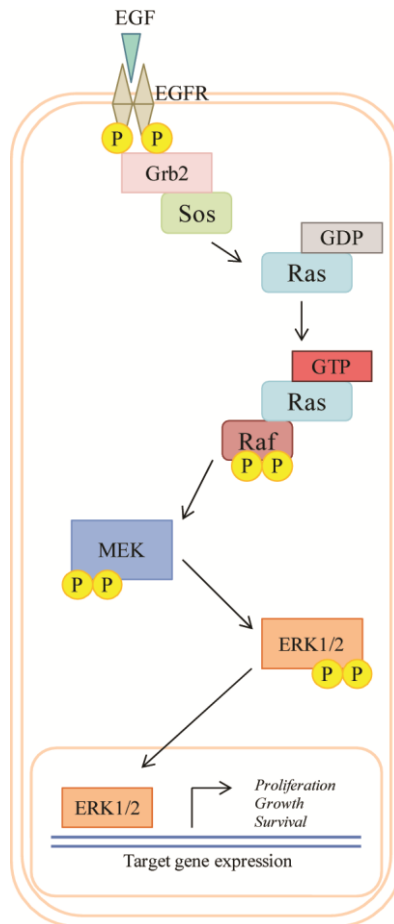
Figure 2. Schematic drawing of the EGFR-RAS-MAPK pathway. The EGFR pathway is activated by EGF binding to the receptor, with subsequent recruitment of GRB2 and SOS. SOS further activates RAS which further phosphorylated and activate RAF. RAF activates MEK through phosphorylation which further activates ERK1/2, which subsequently influences the target gene expression.

Additionally, mutations in the *TP53* gene are identified in 50% or more of colorectal cancers, and are among the most common genetic alterations [8, 15]. The tumor suppressor gene encodes for the P53 protein, which is maintaining genetic stability by inducing cell cycle arrest or apoptosis in response to DNA damage [21]. Mutations in the *TP53* gene which causes allelic loss, rearrangements and deletions are observed in human cancers [22]. Together with modifications of oncogenes and tumor suppressor genes do the aberrations in the *P53* gene subsequently lead to malignancy.

The WNT/β-catenin signaling pathway
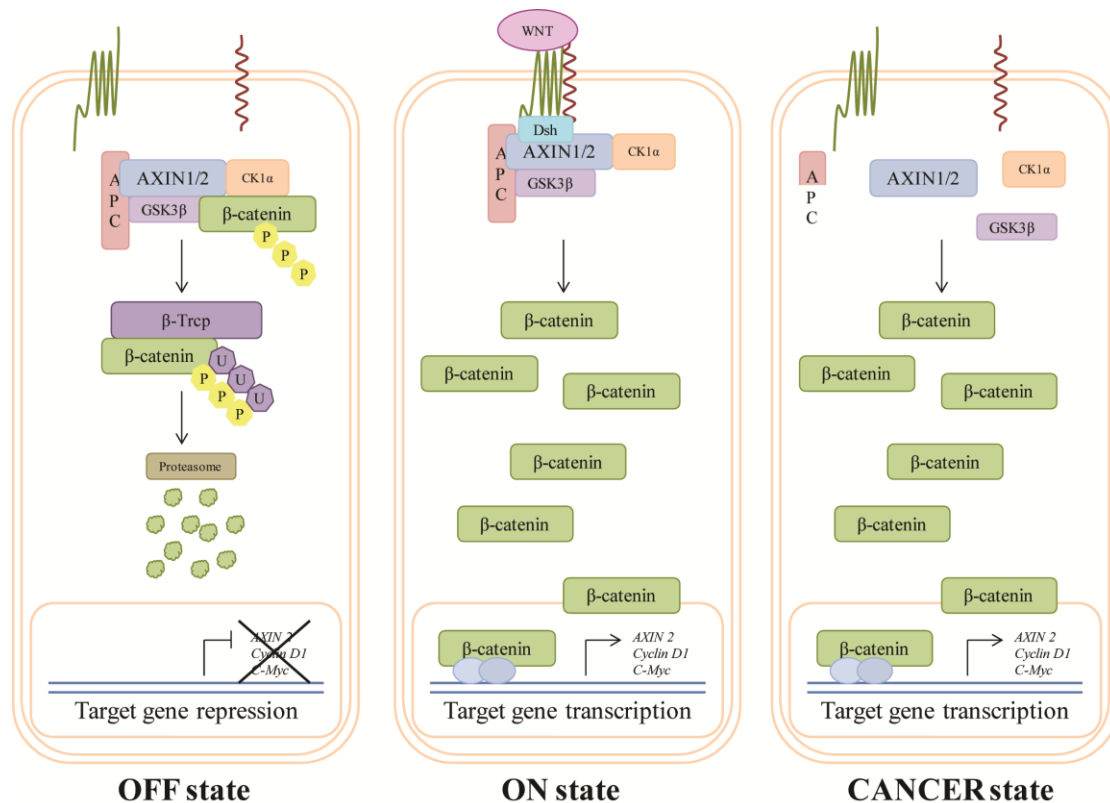
Figure 3. The WNT/β-catenin signaling pathway.
The WNT/β-catenin signaling pathway in "off" state, "on" state and a typical cancer state with APC truncation, leading to a constitutively active pathway.

In naïve cells, the WNT/β-catenin signaling pathway meticulously controls the level of cytoplasmic β-catenin by a protein complex referred to as the WNT/β-catenin destruction complex [23]. The WNT/β-catenin signaling pathway switches between an "on" and "off" state where β-catenin works as a key mediator in WNT signaling transduction, both by binding to transcription factors in the nucleus, and by functioning as a component of epithelial cell adherens junctions at the cell membrane (figure 3) [24]. The β-catenin destruction complex harbors three scaffolding proteins termed AXIN1/2 and APC, which act as scaffolds for the protein kinases casein kinase (CK1α) and the glycogen synthase kinase (GSK3β) [23]. Biochemical studies have reported that AXIN1/2 are the concentration-limiting factor in regulation of the WNT/β-catenin destruction complex's efficiency, with approximately 1000 times lower concentration than the other components of the complex [25]. There are two

AXIN proteins; AXIN1 and AXIN2 [25]. During mouse embryogenesis, AXIN1 was shown to be ubiquitously expressed as an essential component of the β-catenin destruction complex, maintaining low concentration of β-catenin in the cytoplasm. AXIN2 was shown to appear in a more restricted pattern, with increased expression following nuclear β-catenin accumulation, inducing a negative feedback regulation on WNT signaling, thus AXIN2 work as a limiting factor for the duration and intensity of the ongoing WNT signal.

The other scaffolding protein APC is additionally thought to ensure an efficient recruitment and anchoring of β-catenin to the destruction complex on the amino-(N)-terminal domain [23, 26]. When APC is mutated, stabilized AXIN1/2 may be sufficient for maintaining the WNT/β-catenin destruction complex. In this way, CK1α may provide priming phosphorylation of Ser45 on β-catenin, which subsequently enables GSK3β to phosphorylate at Thr41, which in turn primes successive phosphorylation of Ser37 and Ser33 to generate an E3 ubiquitin ligase β-transducin-repeat-containing protein (β-Trcp) binding site [13, 26]. This leads to ubiquitination of β-catenin, and target it for degradation by the proteosome [12]. The suppression of β-catenin clears the T-cell factor (TCF)-lymphoid enhancer factor(LEF) promoters in the nucleus, giving free binding possibilities for Groucho proteins to repress the transcription of WNT target genes [23, 27]. This action will normally keep the levels of cytoplasmic β-catenin low, but when a WNT ligand interact with members of the Frizzled (FZD) family of seven-pass transmembrane proteins with the single-pass transmembrane proteins, low density lipid receptor (LRP)-5 or LRP6, a rapid activation ("on" state) of the WNT/β-catenin pathway occurs [23]. WNT proteins contain a signal sequence with a following highly conserved distribution of cysteines. It has been demonstrated that the FZD protein on the surface of the target cell is the primary receptor for WNT ligand binding [26].

In the activated WNT/β-catenin pathway the combination of WNT ligand, FZD and LRP triggers phosphorylation of Dishevelled (DVL) proteins, which subsequently promote interaction with FZD. The DVL/FZD complex stimulates formation of LRP6 aggregates at the membrane, with further phosphorylation of LRP6s intracellular tail by CK-1γ. This phosphorylation leads to recruitment of AXIN1/2 to the receptor complex, which consequently dissolves the WNT/β-catenin destruction complex, and

β-catenin accumulates in the cytoplasm and in the nucleus [12]. The stabilized pool of β-catenin is further imported in to the nucleus where it interact with the TCF/LEF consensus binding site, and converts them to act as potent transcriptional activators, inducing transcription of WNT target genes, such as *AXIN2, C-MYC* and *CCND1* [12, 23, 25, 27].

As previous mentioned, aberrant WNT/β-catenin pathway signaling are known to play a significant role in human cancers, and is an early progression event in 90% of colorectal cancers [28]. Mutations in WNT pathway components, as APC-, β-catenin- or AXIN1/2 enables a ligand-independent "on"-state of the WNT/β-catenin signaling pathway, which leads to a constant abundance of free β-catenin in the nucleus. Because of the high pathway activity implicated in most cases of CRC, the pathway is attractive for anticancer therapies. However, development of WNT pathway inhibitors has been problematic due to the limited number of suitable pathway components [29]. However, Huang and colleagues discovered that tankyrase1 (TNKS1/PARP-5a/ARTD5) and tankyrase2 (TNKS2/PARP-5b/ARTD6) both interacted with a highly conserved domain of AXIN1/2, which subsequently lead to degradation through the ubiquitinin-proteosome pathway. In this way, TNSK1/2 works as a target for WNT signaling pathway therapies [29, 30].

Tankyrase

Tankyrase is a member of the poly(ADP-ribose) polymerase (PARP) family, which is subdivided into mono(ADP-ribosyl)ating and poly(ADP-ribosyl)ating (PARP) proteins [30]. TNKS1 and TNKS2 (figure 4) belong to the PARP polymerases and uses adenosine diphosphate (ADP) ribosylation as a catalytic process to modify proteins [30]. This is accomplished by using nicotinamide adenine dinucleotide (NAD$^+$) as a substrate to create post-translational modifications on the amino acid side-chains to the acceptor protein.
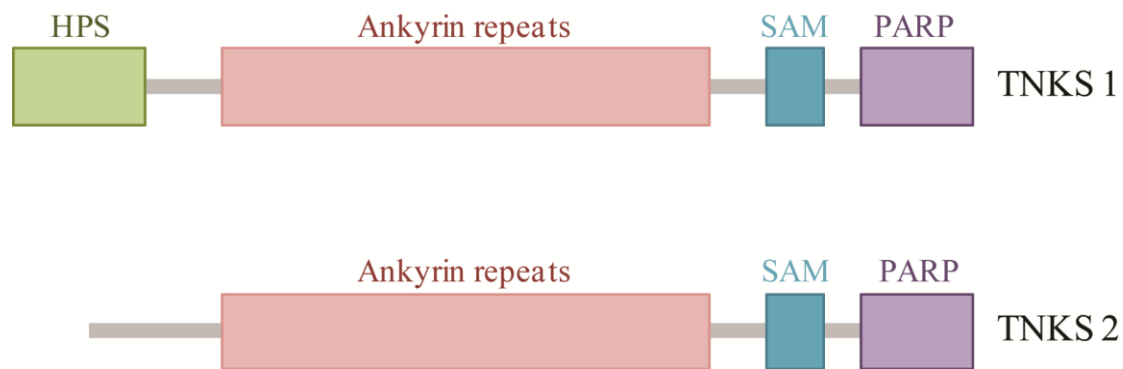
Figure 4. Schematic drawings of the TNKS1 and TNKS 2

TNKS1 has a region with homopolymeric runs of His, Pro and Ser (HPS domain aa 1-181), followed by 15 Ankyrin repeats (aa 215-934), the sterile alpha motif (SAM) at aa 1030-1089, and the PARP catalytic domain at aa 1112-1317. TNKS2 is identical to TNKS1 except for the HPS domain.

In contrast to other PARPs, TNKS1/2 contain several ankyrin repeats and a sterile alpha motif (SAM), where the ankyrin repeats create the interaction with the target protein, and the SAM domain configure the multimerization of the tankyrases [31]. In addition both TNKS1/2 contain the the catalytic poly-ADP polymerase (PARP) domain which is known as an automodification- and DNA binding domain [32].

An important function of TNKS1/2 is to regulate AXIN1/2 by PARsylation (figure 5). PARsylated AXIN1/2 is recognized by a RING-domain E3 ubiquitin ligase named Ring Finger protein 146 (RNF146), which further promotes degradation of the AXIN1/2 protein, and disassembly of the WNT/β-catenin destruction complex [33].

In addition, TNKS1 is identified as a binding partner for telomerase repeat binding factor 1 (TRF1), which plays an important role regulating the telomere length at the chromosome ends [34]. However, the relation between telomere regulation and WNT/β-catenin signaling is not fully understood [34]. Up-regulation of TNKS1 is also shown to correlate significantly with highly aggressive disease with poor prognosis in cancers like breast-, colon- and bladder cancer, and due to this TNKS1 is seen as a potential therapeutic target [35].

Tankyrase inhibition

In 2009, a small molecule XAV939, was developed which stimulated β-catenin degradation by stabilizing AXIN1/2 in the WNT/β-catenin destruction complex [29]. Further analysis with chemical genetic screening showed that XAV939 selectively inhibited β-catenin-mediated signaling by binding to the catalytic PARP domain of TNKS1/2, which lead to stabilization of AXIN1/2 in the WNT/β-catenin destruction complex [29] [35]. In addition, they found down-regulation of cyclin D1 and c-Myc proteins, which are downstream target proteins of β-catenin, which verified prevention of WNT/β-catenin signaling [35].
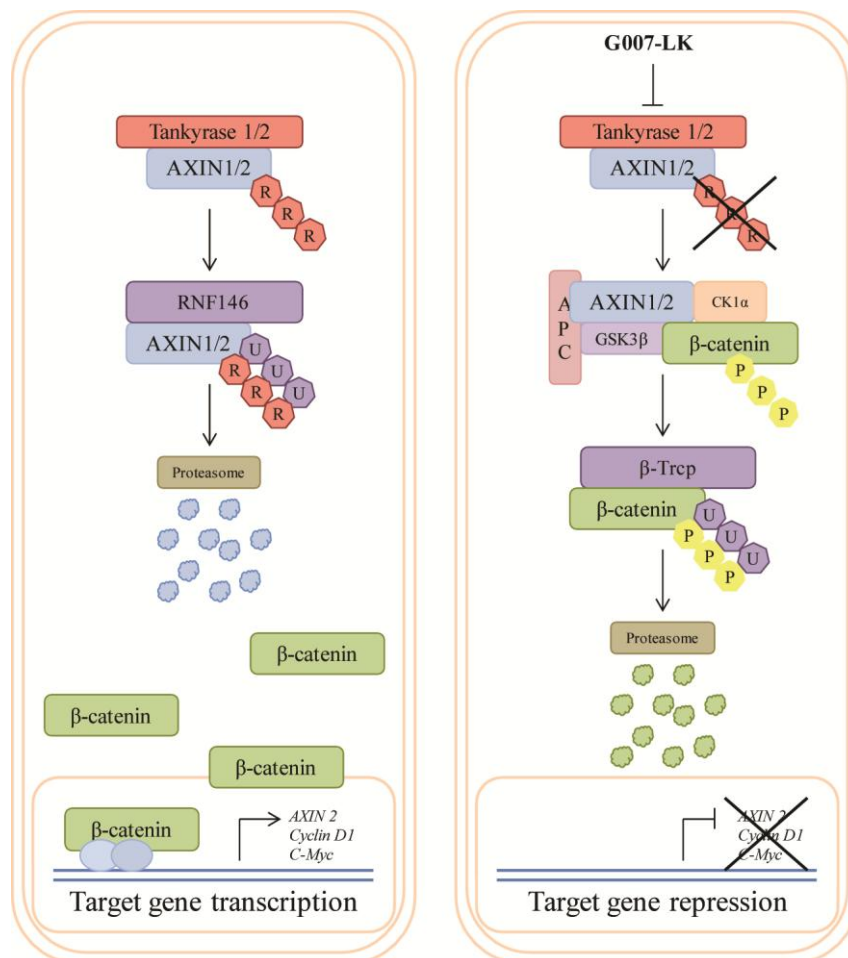
Figure 5. The effect of tankyrase inhibition. The activation of the WNT/β-catenin signaling pathway due to AXIN1/2 inhibition by TNKS1/2, and how inhibition of TNKS1/2 by G007-LK stabilizes AXIN1/2 with subsequent reconstruction of theWNT/ β-catenin destruction complex.

Presently, tankyrase inhibitors are classified in two groups; those binding to the nicotinamide pocket of the PARP domain, such as XAV939, and compounds occupying the adjacent adenosine binding pocket as for instance JW 55 and JW74 [30].

Waaler and colleagues identified in 2012 the novel small molecule inhibitor JW55, which through TNKS1/2s PARP domain inhibition created a significant reduction of β-catenin levels *in vitro*, and a massive accumulation of cytoplasmic AXIN2 [36]. Even though the JW55 inhibitor gave substantial increased specificity compared to XAV939, the new inhibitor had additional mechanisms which could induce unspecific intracellular effects upon tankyrase inhibition. Waaler and colleagues identified in addition the compounds JW67 and JW74 as TNKS1/2 inhibitors. These compounds showed great reduction in active β-catenin protein levels in human CRC cells, with subsequent down-regulation of WNT target genes such as *AXIN2, NKD1* and *SP5* [37]. However, for clinical relevance a tankyrase inhibitor was needed with significantly improved selectivity and pharmacokinetic properties compared to existing ones [30]. In 2013, five specific regions of JW74 were selected for further modification, leading to the development of the chemical analog named G007-LK [30]. G007-LK showed increased tankyrase inhibition compared to the initial compound JW74, and had high target specificity, high potency and both *in vitro,* and *in vivo* stability in mice. TNKS1/2 are inhibited by G007-LK due to the specific binding to TNKS`s extended adenosine pocket of the PARP domain.

2. Aim of the study

In this thesis we wanted to investigate whether β-catenin is localized with WNT destruction complex components in the TNKSi resistant HCT-15 cell line. We will compare the results to COLO 320DM sensitive cells where β-catenin is localized with the WNT destruction complex, which result in reduced β-catenin protein levels. We wanted to investigate whether separate pools of destruction complex components prevent β-catenin from localizing with the WNT destruction complex, and thus protect β-catenin from degradation.

3. Materials and Methods

3.1 Cell lines and cultivation

3.1.1 COLO 320DM and HCT-15 cell lines

In this study, the two CRC cell lines COLO 320DM (American type culture collection [ATCC] Cat# CCL-220) and HCT-15 (ATCC, Cat# CCL-225) were used to look at the different regulation of β-catenin in the WNT/β-catenin signaling pathway. The COLO 320DM cells are rounded and refractile, derived from the colon tissue of a 55 year old human female with Caucasian ethnicity. HCT-15 cells have epithelial morphology and are derived from the colon tissue of a human male. Both cell lines derived from Dukes` type C (lymph node(s) involvement) colorectal adenocarcinoma disease [38, 39].

3.1.2 Cell cultivation

The two cell line`s cultural needs were obtained using the base culture medium ATCC-formulated RPMI-1640 Medium, 500 ml (Sigma-Aldrich, Cat# R8758), with a 10% concentration of Fetal bovine serum (Life Technologies, Cat# 16141-079), and 1% "Penicillin/Streptomycin" (Sigma-Aldrich, Cat# P4333). The cell lines were cultivated at 37°C in a humidified chamber containing 5% CO_2. Cells were split 1:10 when they reached 80-85% confluence, which accounted the need for splitting usually twice a week.

3.1.3 Cell splitting

When working with cells, maintenance of the log phase with exponential growth is important to obtain authentic results.

The culture medium was removed and cells were washed with 1X phosphate-buffered saline ([PBS], OUS, Ullevål, mikrobiologisk avdeling). The PBS was replaced with Trypsin-EDTA (Sigma-Aldrich, Cat# T3924) to detach the cells at 37°C for approximately 15 minutes. When cells were completely detached, RPMI-1640

medium was added to inhibit the Trypsin-EDTA activity, and 1:10 was left in the flask prior to addition of new RPMI-1640 medium.

3.1.4 Mycoplasma testing

It is critical to avoid Mycoplasma infections in research cultures since Mycoplasma has been shown to affect cell physiology and metabolism [40].

The MycoAlert^{TM} commercial Mycoplasma Detection Kit (Fischer, Cat# 11680271) was used to test for Mycoplasma infection in the cell supernatant. The Kit works as a selective biochemical test which detects *Mycoplasma, Acholeplasma, Entomoplasma* and *Spiroplasma;* except *Ureaplasma*, which are six of the main Mycoplasma culture contaminants [41]. The test detects the activity of mycoplasmal enzymes through light signal via luciferase enzymes in the Mycoalert^{TM} substrate. Cells in this study were at all time Mycoplasma free.

3.1.5 Inhibitor treatment

G007-LK (ChemRoyal Inc) is received as a powder with a molecular weight at 529,96 g/mol. The substance is further dissolved in Dimethyl sulfoxide ([DMSO], Sigma-Aldrich, Cat# D8418) to create a stock solution of 10 mM, which was further diluted to 1 µM in culture media. 0,01% DMSO was used as treatment control. The GDC-0973 5 mg solution (Med Chem express, Cat#HY-13065) was dissolved in DMSO to create a 3 µM solution. There was additionally used a combination of both 1 µM G007-LK and 3 µM GDC-0973. In these experiments, 0,04% DMSO was used as treatment control.

3.1.7 IncuCyte assay

An IncuCyte FLR 20x (Essen BioScience, Ann Arbor, Michigan, USA) instrument was used to monitor cell confluency over time. 2,000 cells were seeded per well in a 96-well microplate (Nunc^{TM}), and placed at 37°C over night. Next morning the culture media was exchanged with 300 µl culture media containing 1 µM G007-LK or 3 µM GDC-0973, in addition wells with culture media exchanged with 0,01% DMSO

as a control in 3-6 replicates per treatment. The plate was placed in the IncuCyte FLR 20x instrument, were phase-contrast pictures were taken every second hour throughout the experiment. Data was analyzed by the IncuCyte 2011A software (Essen BioScience), and exported to Excel for further analysis and graph design.

3.1.8 Real Time quantitative PCR analysis

Real Time quantitative PCR analysis (RT-qPCR) is a significant method to study expression of specific genes at RNA levels [42]. The assay requires the use of probes designed to recognise and bind to specific RNA transcripts, which further will be quantified by the polymerase chain reaction.

Cells were collected and RNA isolated using the GenElute^{TM} Mammalian Total RNA Purification Kit (Sigma-Aldrich, Cat#RTN350). Next, 1 µg RNA was converted to cDNA using the SuperScript$^{®}$ VILO^{TM} cDNA Synthesis Kit (Life Technologies, Cat#4309849). To create the quantification of specific genes, a mixture of TaqMan Gene Expression Master Mix (Life Technologies, Cat#4309849), cDNA and a selected probe was added to each well of a 84 well MicroAmp Optical 384-Well Reaction Plate with Barcode (Life Technologies, Cat#4370074) with 3 replicates, according to manufacturer. The probes selected in this thesis was *GAPDH* (ID#Hs02758991_gl) as endogenous reference gene, *AXIN2* (ID#Hs01063170_ml) and *CCND1* (ID#Hs00765553_ml). To seal the plate, MicroAmp Optical Adhesive Film (Life Technologies, Cat#4311971) was used before the RT-qPCR reaction was ran in a the ViiA^{TM} Real-Time PCR system (Life Technologies, Cat#4370074) with an amplification protocol sat to 45 cycles, with denaturation for 20 seconds at 95°C and annealing of probes and amplification for 20 seconds at 60°C. The RT-qPCR results was transferred to Excel and analyzed by comparative quantification methods ($\Delta\Delta$CT value).

3.1.9 Statistics

All statistical analysis was performed in Microsoft$^{®}$ Excel Software for both calculations of proliferation graphs, RT-q-PCR expression and Luciferase units. To

investigate statistical significant differences, Student`s t-test, 2 tailed, unequal variance, * = < 0,05 in Microsoft® Excel Software was used.

3.2 Dual-Luciferase Reporter 1000 Assay System

Dual-Luciferase Reporter 1000 Assay System is a type of genetic reporter system that is widely used to study gene expression and cellular physiology in eukaryotic cells [43]. The measured activation of firefly luciferase (*Photinus pyralis*) correlates with the effect of specific experimental conditions. This reaction is then quenched, and *Renilla* luciferase *(Renilla reniforms)* is measured to serve as the baseline response [43].

3.2.1 Dual-Luciferase Reporter 1000 Assay System on transiently transfected cell lines

$1,25 \times 10^6$ COLO 320DM cells and $1,00 \times 10^6$ HCT-15 cells per well were seeded in two separate 6-well plates, and incubated for 24 hours at 37°C. A mix containing FuGENE HD Transfection Reagent (Promega, Cat# E2311), Renilla pRL-TK Vector (Promega, Cat# E2241) and the Super Top-Flash pTA-Luc Vector which were a gift to Stefan Krauss` laboratory from RT. Moon [44], was mixed well, and applied to the cells. The plates was incubated at 37°C over night.

Table 1. Transfection mixture with vectors and FuGENE® HD Transfection Reagent used to transiently transfect COLO 320DM and HCT-15 cells.

Transient Transfection with FuGENE HD	
Medium to a final volume of	2 ml
STF DNA amount	5 µg
Renilla DNA amount	0,05 µg
Volume of FuGENE® HD Transfection Reagent	16 µl in 550 µl Optimem

24 hours after transfection, cells were dissociated and 1,000 cells were plated per well in a 96-well Nunc plate. The next day, culture media was changed with 0,01% DMSO and 1 μM G007-LK treatment for 72 hours, with 3 replicants. The Dual-Luciferase Reporter Assay 1000 assay kit (Nerliens Meszansky, Cat# E1980) was used according to the manufacturers protocol and luciferase activity was measured with the GloMax®-Multi Detection System (Promega, Cat# E4861).

3.3 RNA interference with esiRNA

Endoribonuclease-prepared small interfering RNAs (esiRNA) are pools of short double-stranded RNAs that through the RNA-induced silencing complex (RISC) works as a template to recognize complementary transcripts, and thereby control the gene expression by causing a knock down effect [45].

3.3.1 Transfection with esiRNA

$1,25 \times 10^6$ COLO 320DM cells, and $1,00 \times 10^6$ HCT-15 cells were plated per well in a 6 well plate. The plates were incubated at 37°C over night, before the RPMI-1640 medium was changed to 1,8 ml RPMI-1640 medium without Penicillin/Streptomycin. The cells were transfected with a final concentration of 40 nM esiRNA in 2 ml medium, which constituted the amount of 5,8 μl esiRNA. Two Eppendorf tubes were blended; One with 5,8 μl esiRNA and 100 μl Opti-MEM (Invitrogen, Cat# 31985-047) per well to be transfected. Optimem and Lipofectamine were incubated for 5 minutes in room temperature before the two tubes were mixed. The mix was incubated for 20 minutes at room temperature to allow formation of Lipofectamine/esiRNA complexes. 200 μl solutions were carefully added to each well, and the cells were incubated at 37 °C for 72 hours.

Table 2. All esiRNA with catalog number and producer.

Product	Producer	Catalog nr.
APC esiRNA	Sigma-Aldrich	EHU079171
AXIN 1 esiRNA	Sigma-Aldrich	EHU073901
AXIN 2 esiRNA	Sigma-Aldrich	EHU001481
β-catenin esiRNA	Sigma-Aldrich	EHU139421
GSK3α esiRNA	Sigma-Aldrich	EHU040791
GSK3β esiRNA	Sigma-Aldrich	EHU079451
EGFP esiRNA	Sigma-Aldrich	EHUEGFP

3.3.2 Western Blot

Western blotting is a technique in cell and molecular biology, which makes it possible to identify specific proteins from a mixture of proteins, by separating them based on molecular weight through gel electrophoresis, producing preferably one band for each protein [46].

The cells were lysed with 1X Pierce® RIPA Lysis buffer (Thermo Scientific, Cat# 89901), containing cOmplete Tablets – Protease inhibitor Cocktail Tablets (Roche applied science, Cat# 4693124001) and PhosSTOP – Phosphatase inhibitor Cocktail Tablets (Roche applied science, Cat# 04906837001). Cell lysates were collected with a cell scraper (Sarstedt, Cat# 83.1832) into cold 1,5 ml tubes and incubated on ice for 30 minutes to allow complete lysis of cells. The lysates were subsequently centrifuged at 2°C at $14{,}8 \times 10^3$ RPM for 20 minutes in a tabletop centrifuge, and the supernatant was transferred into a new cold 1,5 ml tube. The Pierce BCA Protein Assay kit (Life Technologies, Cat# 23227) was used to measure the protein concentration according to the manufacturer's instructions. Absorbance was measured at 562 nm in the Emax® Plus Microplate Reader (Molecular devices,Sunnyvale, CA, USA). The absorbance was further calculated to protein concentration based on a BCA standard curve, which include a range from 0-2 µg/ml protein. 15-20 µg protein was diluted to a total volume of 20 µl with distilled H2O, and 5 µl 5X SDS loading buffer was added to get equal concentration.

Table 3. contents of 5X SDS loading buffer

5X SDS loading buffer		
0,6 ml	1 M Tris-HCl (ph 6,8)	(Sigma-Aldrich, Cat# T-3253)
5 ml	50% Glycerol	(Sigma-Aldrich, Cat# G5516-1L)
2 ml	10% Sodium dodecyl sulfate	(Sigma-Aldrich, Cat# L3771-100G)
1 ml	1% Bromophenol blue	(Sigma-Aldrich, Cat# BO126-25G)
0,5 ml	2-mercaptoethanol	(Sigma-Aldrich, Cat# M6250)
0,9 ml	H2O	

Next, the samples were added to a Novex electrophoresis chamber (Life Technologies) with a NuPAGE® 3-8% Tris-Acetat protein gel (Life Technologies, Cat# NP0321BOX) and NuPAGE® Tris-Acetat SDS Running Buffer (Life Technologies, Cat# LA0041) or a NuPAGE® Novex® 4-12% Bis-Tris Protein gel (Life Technologies, Cat# EA0375BOX) with NuPAGE® MOPS SDS running buffer (Life Technologies, Cat# NP0001). PageRuler Prestained Protein Ladder (Thermo Fischer Scientific, Cat# 26616) was loaded in the first well, and then the protein sample was loaded in the following wells. The electricity was sat to 60-90 V to stack the gel, and further 100-120 V to separate the proteins.

An Immobilon® - P^{SQ} PVDF Transfer Membrane (Merck Life Science/Millipore, Cat#ISEQ00010) was activated in Methanol (VWR, Cat#20903.368) for approximately 25 seconds, and incubated in 1X Transfer buffer (3,03 g Trizma-base (Sigma-Aldrich, Cat# T1503) and 14,4 g Glycine (Sigma-Aldrich, Cat# G7126) 200 ml Methanol, and dH$_2$O to a total volume at 1 L) at least 10 minutes before use. Extra thick blot paper (Bio-Rad Laboratories, Cat#1703960) was wetted in 1X Transfer buffer, and further placed in a Trans-Blot® SD Semi-Dry electrophoretic transfer cell (Bio-Rad, Hercules, California, USA) with the activated PVDF Transfer membrane on top, then the protein gel, and a second pre-soaked blot paper on top, to transmit the proteins from the gel to the membrane. Excess fluid and air was removed before transfer at 25 V for one hour.

After transferring the proteins, the PVDF membrane was blocked with milk solution of 5% Nonfat dried milk (AppliChem, Cat#A0830,0500) in TBS-T (Tris buffered saline (TBS) tablets, Medicago, Cat# 09-7510-100) in distilled H_2O) for 20-60 min in room temperature, before incubating the PVDF membrane with primary antibody solution – containing an antibody diluted in TBST – over night at 4°C.

Table 4. Primary antibodies with used dilution, catalog number and producer.

Target protein	Species	Dilution/TBS-T	Catalog nr.	Producer
Primary antibodies				
ACTIN	Rabbit	1:4,000	A2066	Sigma-Aldrich
Active β-catenin (ABC)	Rabbit	1:5,000	8814	Cell signaling Technology
β-catenin	Mouse	1:2,000	610154	BD Bioscience
GAPDH	Mouse	1:4,000	Sc-32233	Santa Cruz Biotechnology
GSK3α	Rabbit	1:1,000	4337	Cell signaling Technology
GSK3β	Rabbit	1:1,000	9315	Cell signaling Technology

The PVDF membrane was relocated in TBS-T and washed approximately 3 x 5 minutes, before a HRP conjugated secondary antibody solution – cooperating with the primary antibody solution – was incubated for one hour in room temperature.

Table 5. HRP conjugated secondary antibodies with used dilution, catalog number and producer.

Target protein	Dilution/TBS-T	Catalog nr.	Producer
HRP conjugated secondary antibodies			
Chicken Anti Mouse	1:10 000	Sc-2954	Santa Cruz Biotechnology
Chicken Anti Rabbit	1:10 000	Sc-2955	Santa Cruz Biotechnology

Before placing the PVDF membrane in the BioRad ChemiDoc^{TM} Touch Imaging System machine (BioRad, Cat#1708370), Amersham^{TM} ECL^{TM} Prime Western Blotting Detection Reagent (GE Helthcare Amersham, Cat#RPN2236) was added to the membrane. Then the HRP conjugated bound secondary antibodies could be detected the through chemiluminiscence, which made it possible to visualize, verify and validate the results [47].

3.3.3 Immunostaining
Immunostaining is a molecular method using fluorescently labeled antibodies to detect and localize specific proteins within cells or tissues [48].

Precision cover glasses (VWR, Cat#MARI0117580) was pre-coated with 1:10 diluted Poly-Lysin (Sigma-Aldrich, Cat#P8920) for 20 minutes, and washed twice with 1X PBS. The glasses were air dried for two hours, followed by UV-light sterilization for 15 minutes. Cells were distributed on the glasses with 0,04% DMSO, 1 μM G007-LK, 3 μM GDC-0973 and a combination of 1μM G007-LK with 3 μM GDC-0973 treatments and incubated at 37°C for 24 hours.

Prior to antibody incubation, cells were fixed with ice cold 4% Paraformaldehyd (Paraformaldehyd powder (Fisher, Cat#04042) in Sodium hydroxide (VWR, Cat#1.06462.5000)) for 15 minutes. The cells were washed twice with 1X PBS before permabilization with 0,1% Triton X-100 (Roche applied science, Cat#10 789 704 001) in PBS for 15 minutes.

A selected primary antibody diluted in 4% BSA/PBS (BSA Cohn faction V, Proteasfri (Saveen Werner AB, Cat#B2000-100)) was applied to the cells for 1 hour at room temperature (or overnight at 4°C). When using β-catenin mouse primary antibody, TNKS1/2 rabbit primary antibody was selected. While when using AXIN2, GSK3α or GSK3β rabbit primary antibody, TNKS1/2 mouse antibody was selected.

Table 6. Primary antibodies with used dilution, catalog number and producer.

Target protein	Species	Dilution	Catalog nr.	Producer
Primary antibodies				
APC	Mouse	1:50	Sc-9998	Santa Cruz Biotechnology
AXIN 2	Rabbit	1:50	2151	Cell signaling Technology
β-Catenin	Mouse	1:500	610153	BD Bioscience
GSK3α	Rabbit	1:100	4818	Cell signaling Technology
GSK3β	Rabbit	1:100	9315	Cell signaling Technology
TNKS1/2	Rabbit	1:50	Sc-8337	Santa Cruz Biotechnology
TNKS1/2	Mouse	1:50	Sc-365897	Santa Cruz Biotechnology

Cells were washed twice with PBS to remove excess primary antibody solution before incubation with corresponding secondary antibody dilutes in 4% BSA/PBS for one hour at room temperature.

The cells were rewashed before a Fluoroshield with DAPI (1 µg/ml) (Sigma-Aldrich, Cat#F6057) was left on for five minutes at room temperature. Finally, the cover glasses was mounted on Microscope slides (Marienfeld, Cat#10000200) with ProLong® Diamond Antifade Mountant (Life Technologies, Cat#P36965), and placed at 4°C, in dark, until use.

Table 7. Secondary antibodies with used dilution, catalog number and producer.

Target protein	Dilution	Catalog nr.	Producer
Secondary antibodies			
Goat Anti Mouse Alexa Fluor 488	1:500	A11001	Life Technologies
Anti Mouse Alexa 594	1:500	A11005	Life Technologies
Anti Rabbit Alexa 488	1:500	A21206	Life Technologies
Anti Rabbit Alexa 594	1:500	A11012	Life Technologies

4. Results

The general localization of WNT/β-catenin destruction complex components
The poly(ADP-ribose)polymerase TNKS1 and TNKS2 are implicated as positive regulators of the WNT/β-catenin signaling pathway by its PARsylation activity which promote AXIN1/2 degradation, and inhibition of the WNT/β-catenin destruction complex [29]. By inhibiting TNKS1/2, an accumulation and stabilization of AXIN1/2 occur, where recent research report that the two AXIN proteins may not be as functionally equivalent as initially demonstrated [49]. AXIN1 is suggested to promote signalosome formation, and thus play an important role in WNT pathway activation, whereas AXIN2 reduces WNT signaling activity, upon tankyrase inhibitor treatment, by promoting β-catenin degradation.

Previous data has demonstrated the lack of influence on both proliferation rate and β-catenin regulation upon tankyrase inhibition in HCT-15 cells [50]. To confirm these observations, an immunofluorescent staining analysis was conducted, detecting the subcellular localization of TNKS1/2 and β-catenin, since β-catenin has been shown to accumulate in TNKS1/2 containing puncta upon tankyrase inhibition [51]. Laser Whitefield microscopy pictures of cells stained with TNKS1/2 (rabbit) antibody (red) and β-catenin (mouse) antibody (green) revealed a significant difference in protein localization between the two cell lines. In COLO 320DM cells treated with control media (DMSO), β-catenin was predominantly localized in the nucleus while TNKS1/2 was localized in the cytoplasm (figure 6a). In HCT-15 cells treated with control media, both β-catenin and TNKS1/2 were localized in the cytoplasmic membrane, however the two proteins did not co-localize. In COLO320DM cells, 1 µM G007-LK treatment (tankyrase inhibition;TNKSi) induced cytoplasmic clusters containing both β-catenin and TNKS1/2, suggesting an interaction between both proteins. In accordance, immunofluorescent staining assay showed an overall reduction in β-catenin levels, including in the nucleus. In HCT-15 cells, TNKSi induced TNKS1/2 containing protein clusters in the membrane; however, these clusters did not contain measurable levels of β-catenin. Hence, the lack of β-catenin degradation in this cell line may be due to a lack of physical interaction between the two proteins.
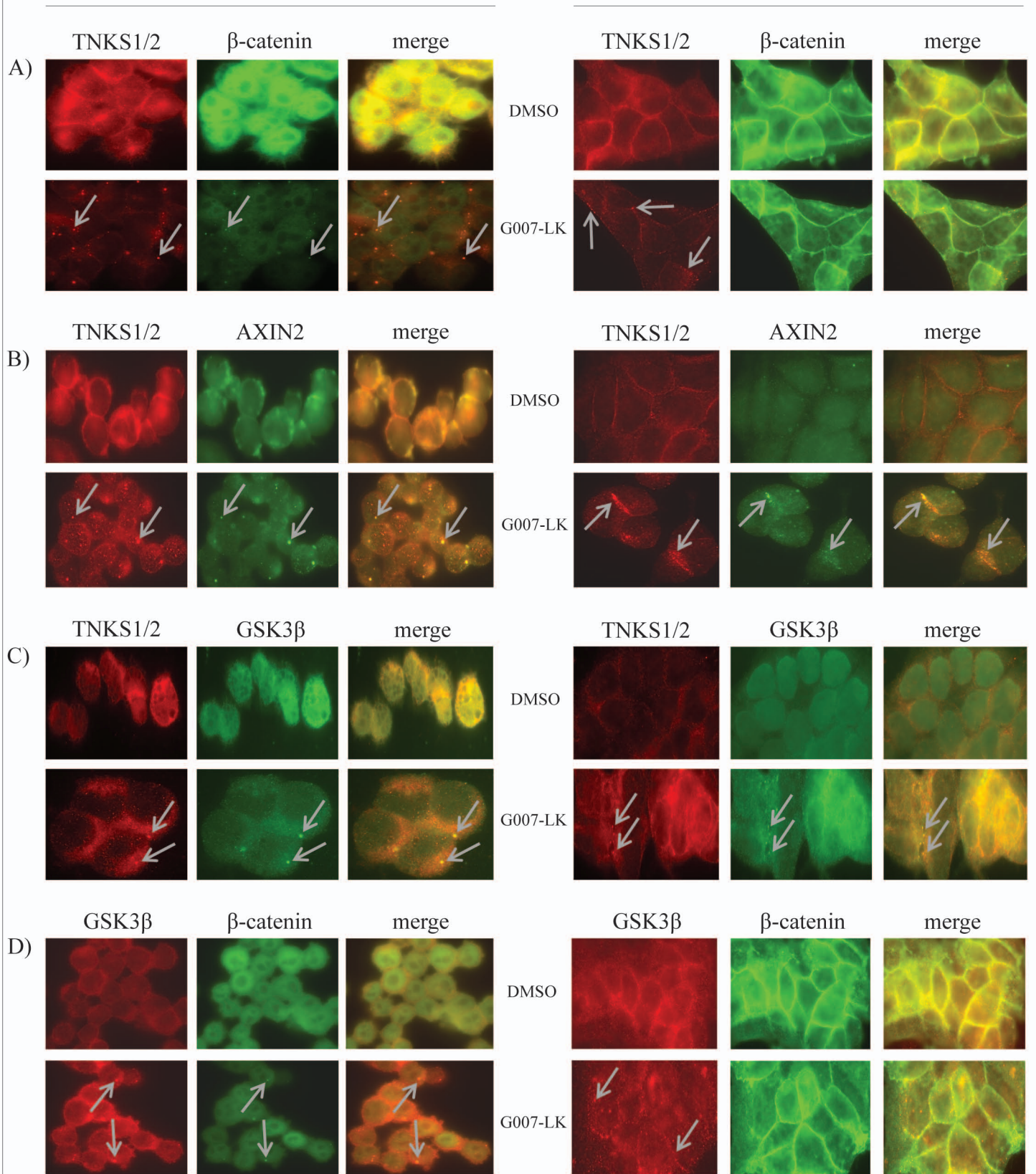
Figure 6. General localization of β-catenin destruction complex components. A representative selection of laser Whitefield microscopy pictures of COLO 320DM and HCT-15 colorectal cancer cells, 63 X magnified, treated with 0,01% DMSO (top) and 1 μM G007-LK (bottom) for 24 hours, and immunostained with antibodies against TNSK1/2, β-catenin, GSK3β and AXIN2. A) Cells stained with TNKS1/2 (red, rabbit 1°ab) and β-catenin (green, mouse 1°ab). B) TNKS1/2 (red, mouse 1°ab) and AXIN2 (green, rabbit 1°ab). C) TNKS1/2 (red, mouse 1°ab) and GSK3β (green, rabbit 1°ab). D) GSK3β (red, rabbit 1°ab) and β-catenin (green, mouse 1°ab). Arrows points to clusters referred to as β-catenin destruction complexes.

Next we wanted to investigate whether TNKS1/2 was co-localized with other components of the WNT/β-catenin destruction complex, like GSK3β and AXIN2 in HCT-15 cells compared to COLO 320DM cells, or whether GSK3β was located with β-catenin. Thus, an immunofluorescent staining was conducted using TNKS1/2 (mouse) antibody (red) with AXIN2 (rabbit) antibody (green) (figure 6b), TNKS1/2 (mouse) antibody (red) with GSK3β (rabbit) antibody (green) (figure 6c) and GSK3β (rabbit) antibody (red) with β-catenin (mouse) antibody (green) (figure 6d). In COLO 320DM cells treated with control media, GSK3β and AXIN2 localized predominantly in the cytoplasm and cell membrane, as shown in figure 6b. In HCT-15 cells treated with control media, both GSK3β and AXIN2 seem to be highly located in the cytoplasm and in the nucleus. In COLO 320DM cells upon TNKSi, β-catenin, GSK3β and AXIN2 accumulated in clusters together with TNKS1/2 in the cytoplasm, which reinforces the theory where TNKSi leads to stabilization of the WNT/β-catenin destruction complex in this cell line. In HCT-15 cells TNKSi treatment relocates GSK3β (figure 6b) and AXIN2 (figure 6c) in clusters together with TNKS1/2 in the membrane, which the arrows point to in figure 6. However, β-catenin is not co-localized in the cytoplasmic clusters, detectable in immunofluorescence analysis.
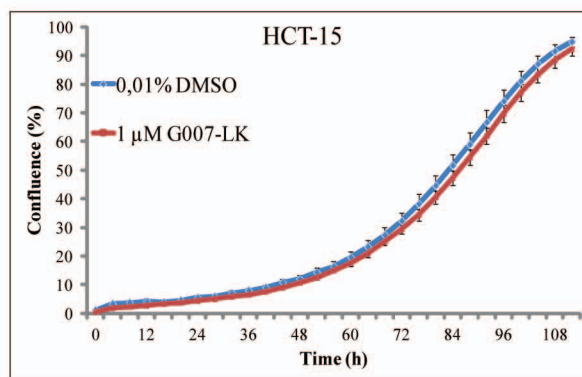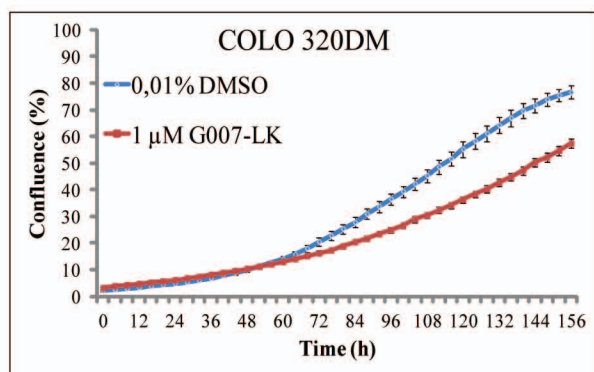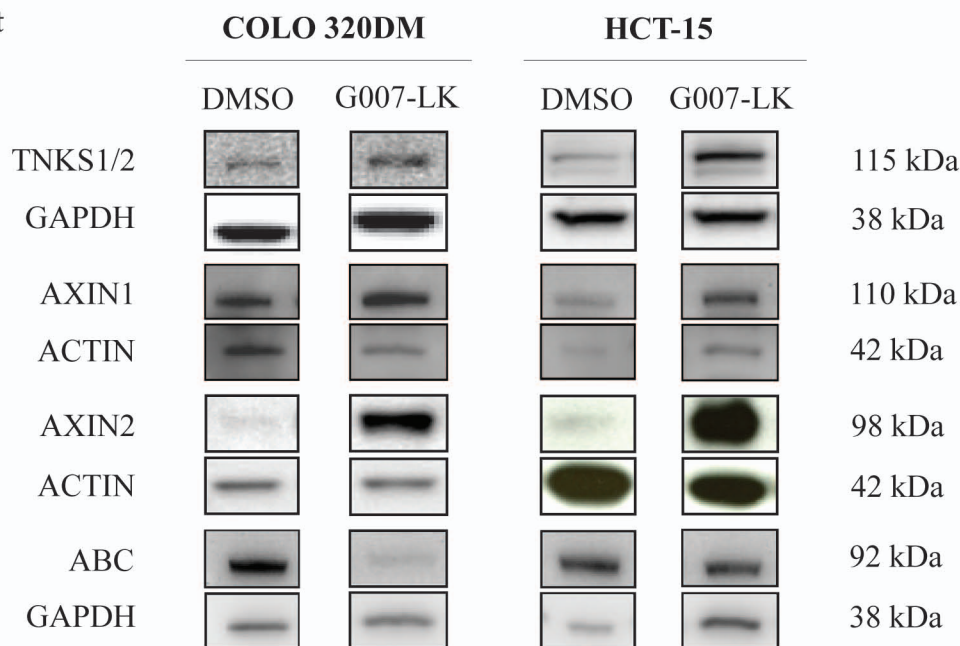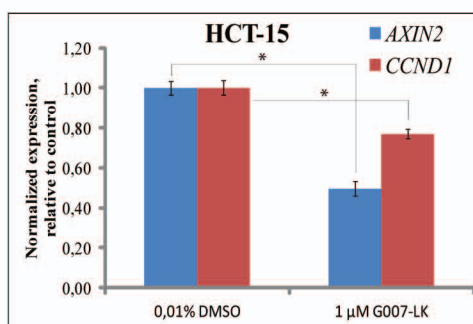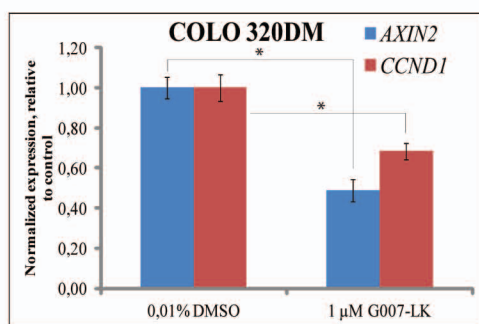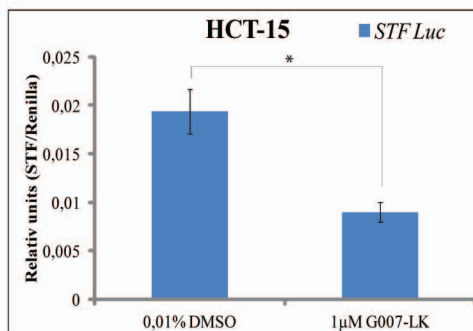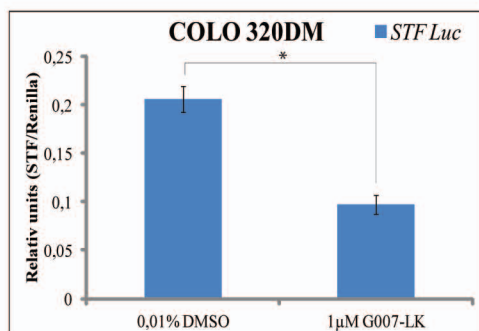
Figure 7. Effect of G007-LK treatment in the two CRC cell lines. A) Representative graphs for both cell lines showing proliferation sensitivity towards 1 μM G007-LK over time as measured by % confluence in an IncuCyte. B) Representative Western blot protein results to estimate TNKSi effect on AXIN1, AXIN2 and ABC protein level, after 24 h treatment with 0,01% DMSO and 1 μM G007-LK. C) Real time quantitative PCR (RT-qPCR) results detecting mRNA levels of 3 replicates of *AXIN2* and *CCND1,* normalized to internal GAPDH expression. D) Luciferase assay detecting *Super Top Flash (STF) Luciferase,* used to detect WNT signaling pathway activity. Bars show relative expression compared to control. Statistics by Student`s t-test, 2 tailed, unequal variance, * = p<0,05

COLO 320DM and HCT-15 CRC cells respond oppositely towards G007-LK tankyrase inhibition treatment

In both COLO 320DM and HCT-15 CRC cell lines TNKSi treatment resulted in up-regulated protein levels of TNKS1/2 (figure 7b), which validates the treatment effect. In COLO 320DM, TNKSi treatment solidly reduced proliferation as measured by IncuCyte live cell analysis system with ~30% of the DMSO control group after 156 hours (figure 7a). This result correspond to the observed co-localization of TNKS1/2/GSK3β/AXIN2/β-catenin with TNKSi (figure 6), and decreased protein levels of Non N-terminal phosphorylated (active) β-catenin (ABC) (Figure 7b). As a complete contrary, no reduction in proliferation was detected upon TNKSi in HCT-15 cells, which may be explained by the absence of β-catenin in the TNKS1/2/GSK3β/AXIN2 membrane clusters, and absence of ABC regulation (figure 7b). Furthermore, TNKSi induced accumulation and stabilization of AXIN1 and AXIN2 protein levels in both cell lines, confirming the uncoupled regulation of AXIN1/2 and β-catenin in HCT-15 cells upon TNKSi.

Since *AXIN2* mRNA levels have been shown to be a direct target of β-catenin in most cell lines, this transcript was used to analyze WNT/β-catenin pathway activity. *CCND1* transcript is known as a cell cycle marker, and is in addition to *AXIN2* a direct target to β-catenin, however also a direct target of other cell cycle regulating proteins. *CCND1* mRNA levels is thus used both to analyze WNT/β-catenin pathway activity and cell cycle influence. In COLO 320DM cells TNKSi reduced *AXIN2* and *CCND1* mRNA levels which correlates with the decrease in ABC protein levels, reduced *STF* activity, and reduced proliferation. In HCT-15 cells, TNKSi similarly reduced *AXIN2* and *CCND1* levels and *STF* activity, although proliferation remained unaffected. The reduction in mRNA transcript is surprising, since TNKSi did not change protein levels of ABC as measured by Western blot and immunofluorescence analysis.
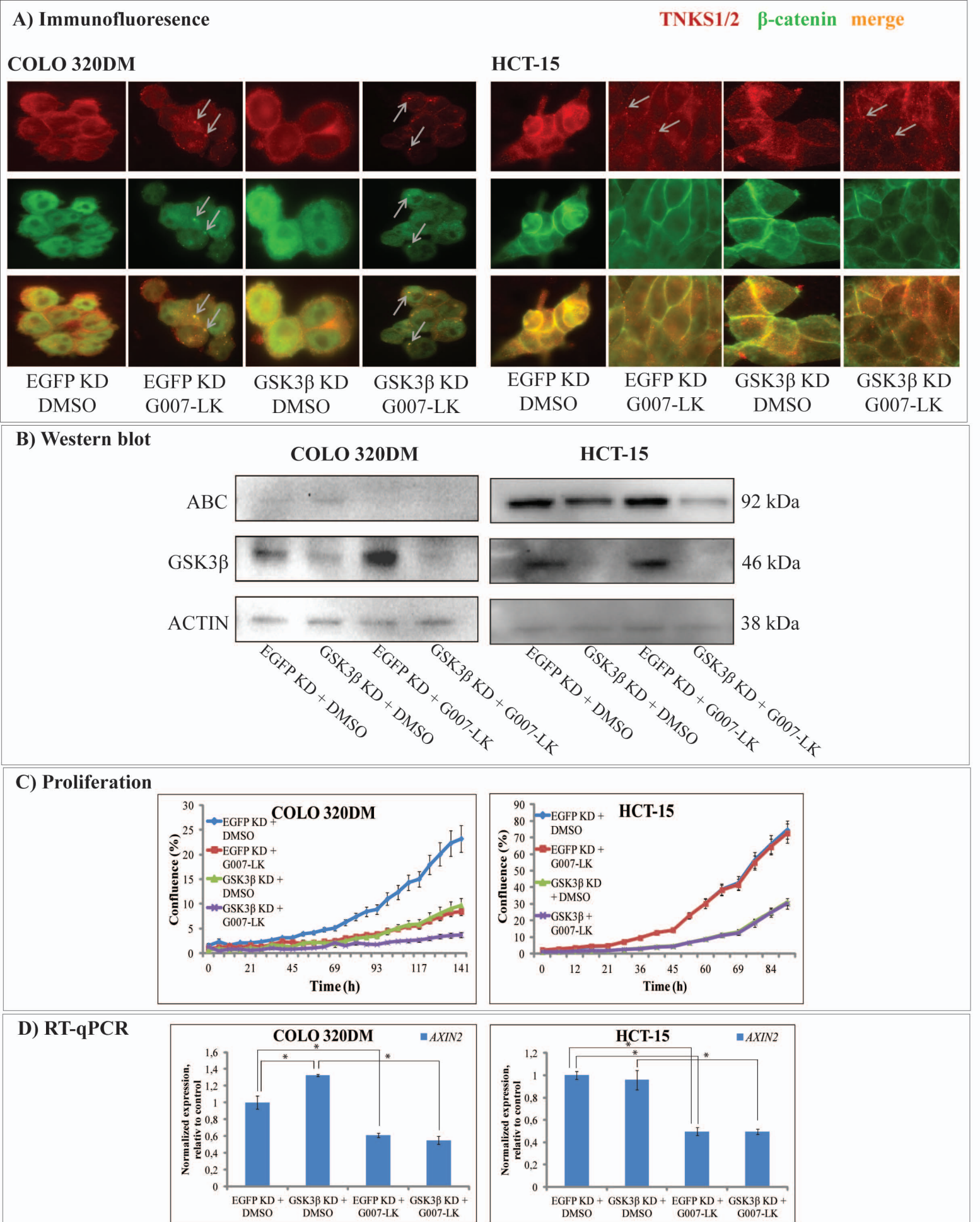
Figure 8. Responses to GSK3β knock down in COLO 320DM and HCT-15 cells. Both cell lines were transfected with EGFP esiRNA (EGFP KD) (control) and GSK3β esiRNA (GSK3β KD) for 72 hours, and treated with 0,01% DMSO (control) and 1 μM G007-LK for 24 hours.
A) Representative laser Whitefield microscopy pictures showing cells stained with antibodies for TNKS1/2 (red) and β-catenin (green).
B) Protein analysis confirming the GSK3β knock down effect in addition to levels of Non N-terminal phosphorylated (active) β-catenin (ABC).
C) IncuCyte assay detecting changes in cell confluence upon GSK3β KD with treatment. Control (EGFP KD + DMSO) (blue),
EGFP KD + G007-LK (red), GSK3β KD + DMSO (green) and GSK3β KD + G007-LK (purple). D) RT-qPCR analysis investigating changes in *AXIN2* and *CCND1* mRNA levels upon GSK3β knock down. All results is normalized to GAPDH and relative to control. Statistical significant differences is validated by Student`s t-test, 2 tailed, unequal variance, * = < 0,05.

Reduced proliferation rate upon GSK3β knock down in both COLO 320DM and HCT-15 cells

Upon TNKSi, there was observed decreased protein levels of ABC in COLO 320DM cells, but no regulation in HCT-15 cells (figure 7b). GSK3β is previous shown to co-localize with TNKS1/2 upon TNKSi (figure 6b), however, we wanted to analyze if GSK3β was forming a complex with β-catenin elsewhere than with TNSK1/2, and if GSK3β esiRNA mediated knock down (GSK3β KD) would lead to relocation of β-catenin with TNKS1/2.

Immunofluorescent analysis of COLO 320DM cells revealed that the GSK3β KD had no visible effect on cellular localization of TNKS1/2 or β-catenin (figure 8a). Upon TNKSi, levels of β-catenin were reduced to the same levels as in the EGFP KD + TNKSi cells, and TNKS1/2 and β-catenin still co-localized in cytoplasmic clusters. In HCT-15 cells, immunofluorescent staining of HCT-15 cells revealed no change in TNKS1/2 or β-catenin levels. GSK3β KD and TNKSi still induced membrane clusters of TNKS1/2, but no co-localization with β-catenin.

Western blot protein analysis validated reduction of total GSK3β protein levels upon the GSK3β KD (figure 8b). In COLO 320DM cells, both control treated (EGFP KD) cells and cells with GSK3β KD induced a reduction in ABC protein levels upon TNKSi, indicating that β-catenin is phosphorylated and degradated even when GSK3β is knocked down. In HCT-15 cells ABC protein levels was reduced with GSK3β KD, independent on TNKSi.

Interestingly, the GSK3β KD dramatically decreased the proliferation rate in both cell lines. In COLO 320DM cells, GSK3β KD mediated similar reduction in proliferation as TNKSi treatment in control (EGFP KD) cells. The combination of GSK3β KD and TNKSi mediated an even lower proliferation rate. In HCT-15, GSK3β KD did not sensitize the CRC cell line to TNKSi, but created a strong decrease in proliferation rate independent of supplemented TNKSi treatment.

The GSK3β KD in COLO 320DM cells treated with control (0,01% DMSO) media showed an increase in *AXIN2* mRNA levels, which validates GSK3β as an important component of the β-catenin destruction complex. When GSK3β is knocked down, β-

catenin will not be degradated and accumulate in the nucleus, where it increases the transcriptional response of WNT/β-catenin target genes. In normal cells, TNKSi treatment stabilizes the WNT/β-catenin destruction complex, and thus prevents β-catenin to accumulate in the nucleus. Interestingly, when combining GSK3β KD with TNKSi, a similar decrease in *AXIN2* mRNA levels occur, indicating that the TNKSi treatment still create down-regulation of β-catenin without the presence of GSK3β. This theory fits together with the proliferation result where combined GSK3β KD and TNKSi created the strongest reduction in proliferation rates (figure 8c). In HCT-15 cells both with and without GSK3β KD, a decrease in *AXIN2* mRNA levels occurred upon TNKSi, meaning that the decrease is independent of GSK3β.

A) Immunofluorescence

COLO 320DM

TNKS1/2

GSK3α

merge

HCT-15

TNKS1/2

GSK3α

merge

EGFP KD + DMSO	EGFP KD + G007-LK	GSK3β KD + DMSO	GSK3β KD + G007-LK

B) Western blot

COLO 320DM   **HCT-15**

GSK3α   51 kDa

GSK3β   46 kDa

GAPDH   38 kDa

EGFP KD + DMSO   GSK3β KD + DMSO   EGFP KD + G007-LK   GSK3β KD + G007-LK   EGFP KD + DMSO   GSK3β KD + DMSO   EGFP KD + G007-LK   GSK3β KD + G007-LK
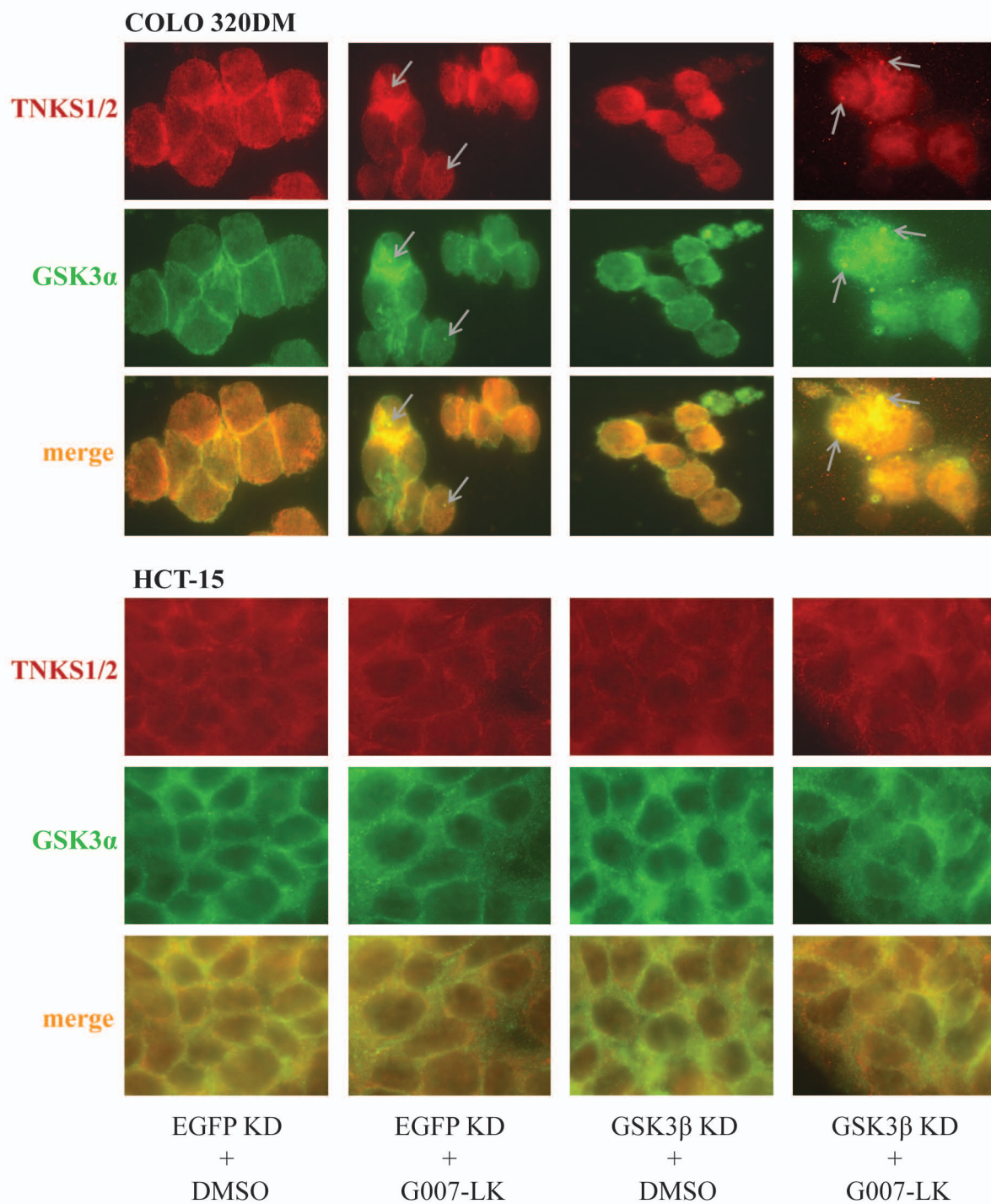
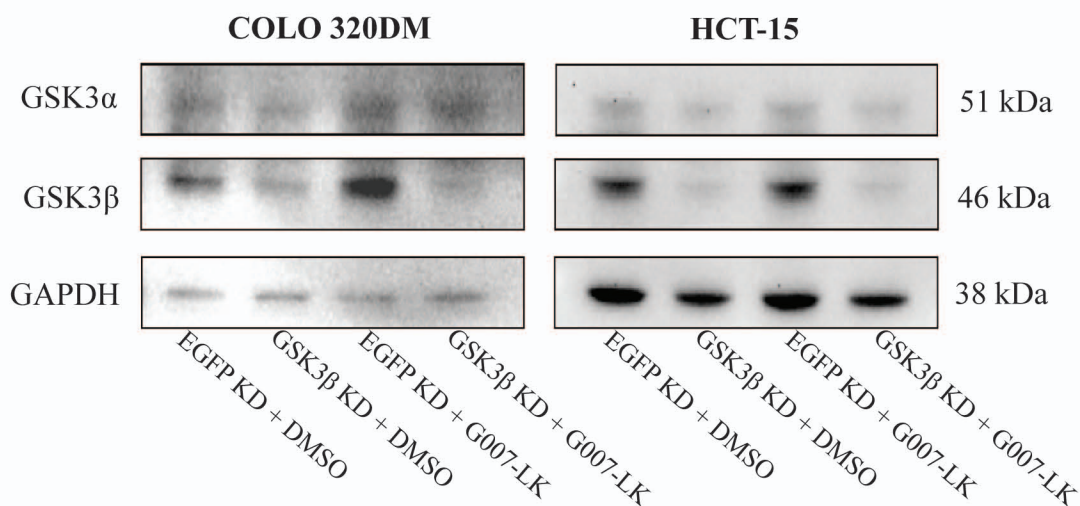**Figure 9. Regulations of GSK3α when GSK3β is knocked down.** A) A representative selection of 63 X magnified laser Whitefield microscopy pictures of COLO 320DM and HCT-15 cells treated with 0,01% DMSO and 1 μM G007-LK for 24 hours, transfected with EGFP esiRNA and GSK3β esiRNA for 72 hours, and stained with antibodies detecting TNKS1/2 (red) and GSK3α (green). B) Protein analysis indicatingexpression of GSK3α upon GSK3β KD.

The functionally redundancy of GSK3α

Due to the lack of change on ABC protein level upon TNKSi and GSK3β KD in COLO 320DM cells, the presence of GSK3α upon GSK3βKD was investigated, since GSK3α has shown to be functionally redundant to GSK3β [52].

In COLO 320DM cells, GSK3α was highly present in both the cell membrane and the cytoplasm (figure 9a). Upon TNKSi, GSK3α was located in cytoplasmic clusters together with TNKS1/2, indicating the presence of GSK3α in the WNT/β-catenin destruction complex. GSK3β KD did not change distribution of GSK3α in COLO 320DM cells independent of treatment. In HCT-15 cells, no visible co-localization between GSK3α and TNKS1/2 was detected, independent of treatment.

Due to poor quality of the antibody, Serine21 phosphorylated (inactive) GSK3α was not detected on Western blot protein analysis, which would have given an indication of change in the proteins activity upon GSK3β KD. However, total GSK3α protein level was detected, indicating increased levels due to TNKSi treatment, both with and without GSK3β presence in COLO 320DM cells (figure 9b). In HCT-15 cells, the levels of GSK3α seem to be unaffected by both TNKSi and GSK3βKD.
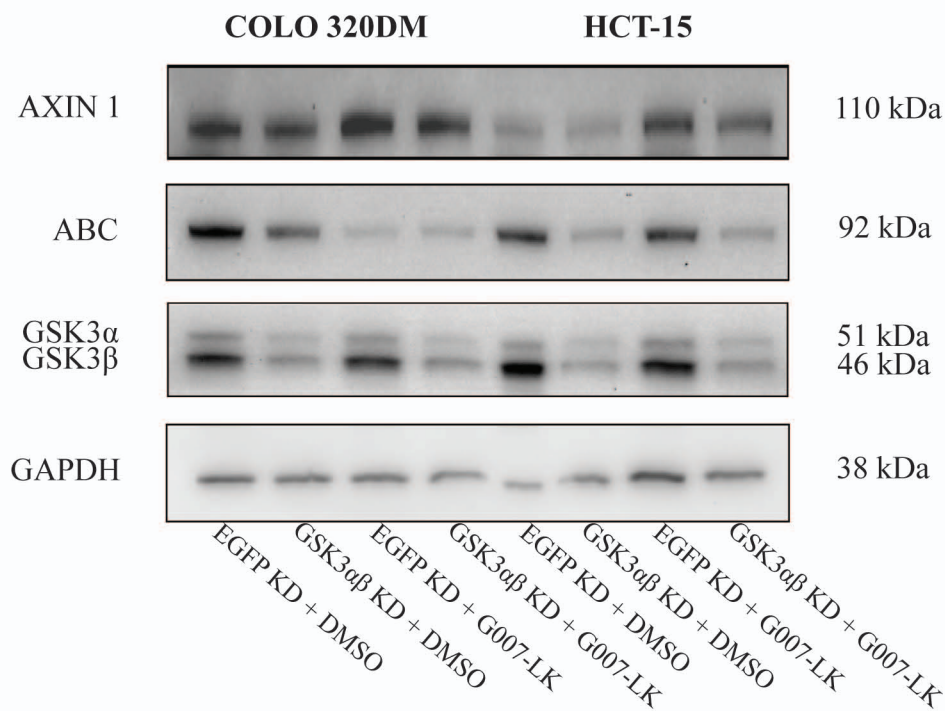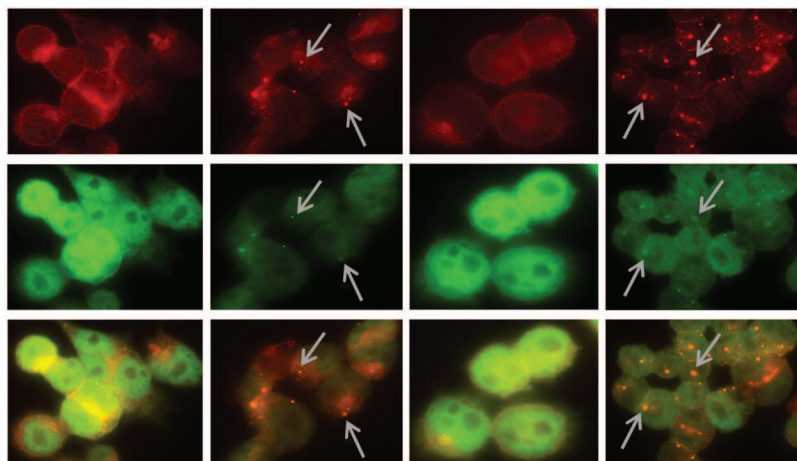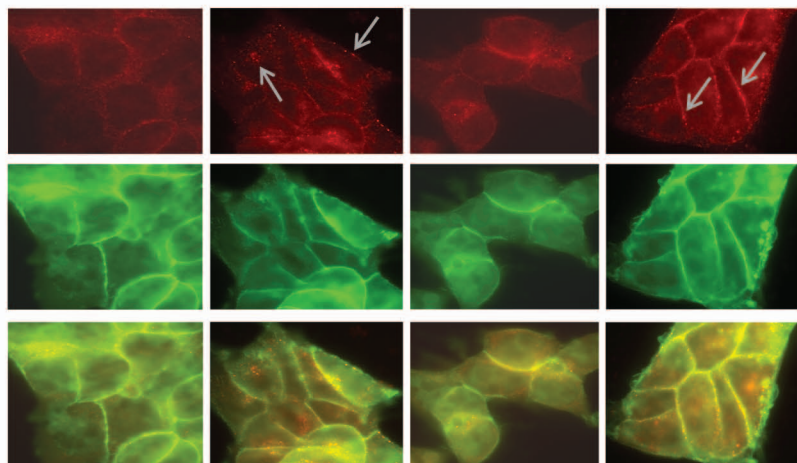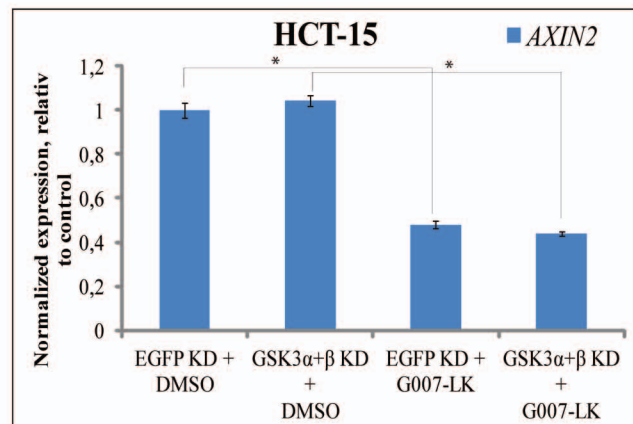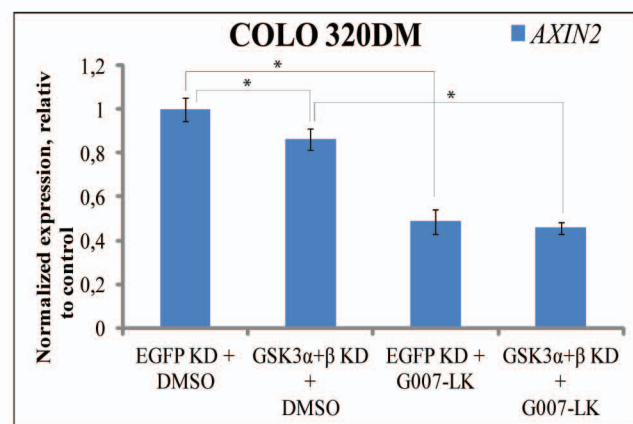
Figure 10. Respons to both GSK3α and GSK3β knock down in COLO 320DM and HCT-15 cells. The cells were transfected with esiRNA for 72 hours, and treated with 0,01% DMSO and 1 µM G007-LK for 24 hours. A) Western blot protein analysis to validate the knock down effect, in addition to look for changes in ABC and AXIN1 levels. B) 63 X magnified Immunofluorescence pictures stained with TNKS1/2 (red) and β-catenin (green) antibodies. C) RT-qPCR analysis validating the affect from GSK3α and GSK3β knock down, on mRNA level. Results are normalized to GAPDH, and relative to control. Statistics by Student`s t-test, 2 tailed, unequal variance, * = p<0,05

A combined knock down assay of both GSK3α and GSK3β

To investigate whether a functional redundancy between GSK3α and GSK3β could explain the lack of effect of the single GSK3β KD, a combined GSK3α and GSK3β knock down was performed, since GSK3α may compensate for GSK3β in the WNT/β-catenin destruction complex.

We wanted to see whether AXIN1 was affected by GSK3α+β KD, since GSK3β regulate AXIN1/2 (figure 10a). However, the knock down created no decrease in AXIN1 protein levels. In addition, protein levels of ABC was detected, revealing similar effects as with single GSK3β KD (figure 8a).

Immunofluorescent staining on COLO 320DM cells treated with DMSO and GSK3αβ KD revealed that TNKSi provided similar co-localized cytoplasmic cluster of TNKS1/2 and β-catenin, even upon GSK3α+β KD (figure 10b). There was additionally detected a valid reduction of ABC protein levels, indicating ongoing degradation (figure 10a). In HCT-15, TNKSi provided TNKS1/2 containing clusters along the membrane, but no co-localization with β-catenin, despite the reduction in ABC protein levels with GSK3α+β KD detected with Western blot analysis.
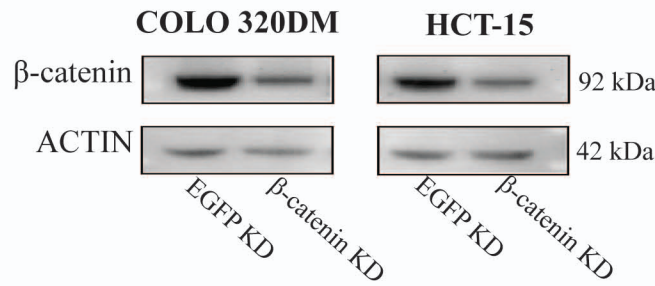
In both cell lines, RT-qPCR analysis of *AXIN2* expressed similar results as with GSK3β KD, revealing that GSK3α+β KD is not regulating *AXIN2* mRNA levels alone upon DMSO treatment. In both cell lines, treatment with TNKSi indeed decreased *AXIN2* mRNA levels, independent of GSK3α+β KD (figure 10c). This highly validate the results in COLO 320DM cells, where ABC protein levels are reduced upon TNKSi, and in immunofluorescent staining assay where β-catenin is present in TNKS1/2 cytoplasmic clusters both with and without GSK3α+β KD. In HCT-15 cells, we observed a TNKSi mediated reduction in *AXIN2* mRNA expression, which was independent of GSK3α+β KD (figure 10c) and despite the different level of decrease in ABC protein levels (figure 10b). Thus, there is reason to believe that the GSK3α+β KD affect ABC protein levels, however β-catenin is not affected through the WNT/β-catenin destruction complex.

A) Western blot

COLO 320DM — HCT-15

β-catenin — 92 kDa
ACTIN — 42 kDa
EGFP KD / β-catenin KD

B) Proliferation

COLO 320DM
- EGFP esiRNA
- β-catenin esiRNA
Confluence (%) vs Time (h)

HCT-15
- EGFP esiRNA
- β-catenin esiRNA
Confluence (%) vs Time (h)

C) Proliferation

COLO 320DM
- EGFP KD + DMSO
- EGFP KD + G007-LK
- β-cat KD + DMSO
- β-cat KD + G007-LK
Confluence (%) vs Time (h)

HCT-15
- EGFP KD + DMSO
- EGFP KD + G007-LK
- β-cat KD + DMSO
- β-cat KD + G007-LK
Confluence (%) vs Time (h)

D) RT-qPCR

AXIN2
COLO 320DM EGFP KD / COLO 320DM β-catenin KD
Normalized expression, relative to control
Untreated, DMSO, G007-LK

AXIN2
HCT-15 EGFP KD / HCT-15 β-catenin KD
Normalized expression, relative to control
Untreated, DMSO, G007-LK

CCND1
COLO 320DM EGFP KD / COLO 320DM β-catenin KD
Normalized expression, relative to control
Untreated, DMSO, G007-LK

CCND1
HCT-15 EGFP KD / HCT-15 β-catenin KD
Normalized expression, relative to control
Untreated, DMSO, G007-LK

Figure 6. β-catenin is not responsible for the proliferation reduction observed with GSK3β in HCT-15 cells. A) IncuCyte proliferation assay with EGFP KD cells and β-catenin KD cells, in culture media. EGFP KD cells in blue line, β-catenin KD cells in red line. B) Western Blot protein analysis result validating the β-catenin knock down effect. C) IncuCyte assay validating changes in proliferation when combining β-catenin KD with TNKSi. D)RT-qPCR analysis detecting mRNA levels of *AXIN2* and *CCND1* transcript, normalized to internal GAPDH expression. Statistics by Student`s t-test, 2 tailed, unequal variance, * = p<0,05.

β-catenin independent proliferation in HCT-15 cells

Next, we wanted to analyze whether the observed down-regulation of β-catenin with GSK3β KD was responsible for the simultaneous reduction in cell proliferation in HCT-15 cells (figure 8). We therefore performed an esiRNA mediated KD of β-catenin (β-catenin KD) in the HCT-15 cell line, and in COLO 320DM cells as control (figure 11a).

In COLO 320DM cells, a strong reduction in proliferation was detected upon β-catenin KD (Figure 11b). This validated the β-catenin dependent proliferation in this cell line. In HCT-15 no statistical relevant change was detected in proliferation rate upon β-catenin KD, which concludes the β-catenin independent proliferation in this cell line.

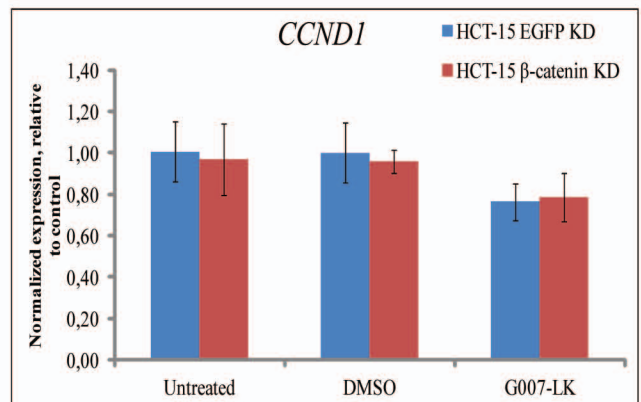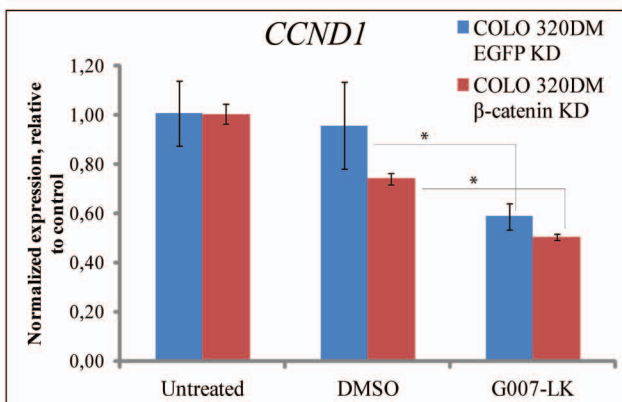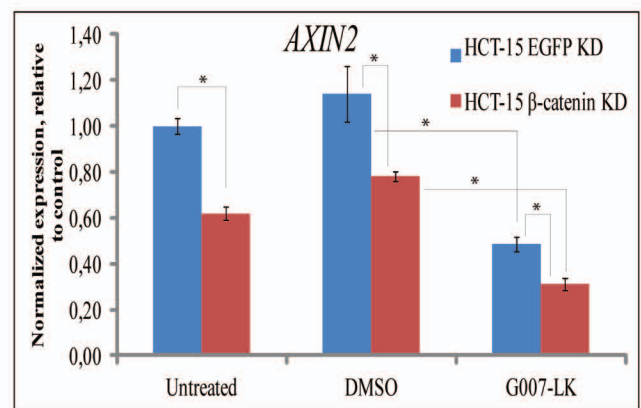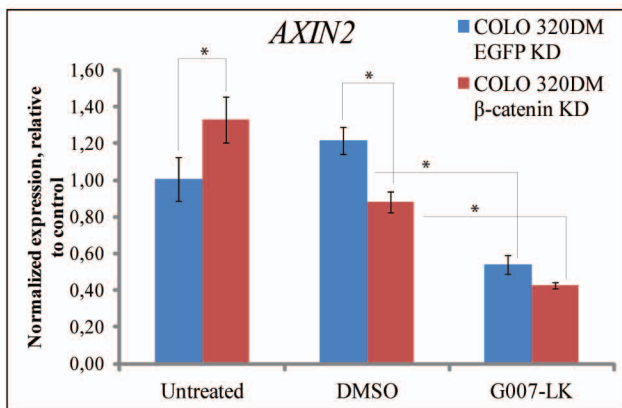In the COLO 320DM cell line TNKSi, at the selected dose, reduced proliferation to similar degree as β-catenin KD, confirming both β-catenin dependent proliferation in this cell line, and the β-catenin degradation mechanism behind G007-LK (figure 11c). Combining β-catenin KD with TNKSi additively reduced proliferation. In HCT-15 cells, sensitivity towards TNKSi was not affected when knocking down β-catenin. In addition, DMSO treatment slightly increased the proliferation rate (of both EGFP KD and β-catenin KD).

In both COLO 320DM and HCT-15 cells with β-catenin KD, the mRNA levels of *AXIN2* and *CCND1* was reduced in the same trend as EGFP KD cells (figure 11d). In HCT-15 cells, levels of *AXIN2* transcript were reduced upon β-catenin KD, which was expected since *AXIN2* is a target gene for β-catenin transcription. Levels of

CCND1 mRNA were not affected by the β-catenin KD, which correlates with the non-affected proliferation rate in this cell line.

A) Proliferation
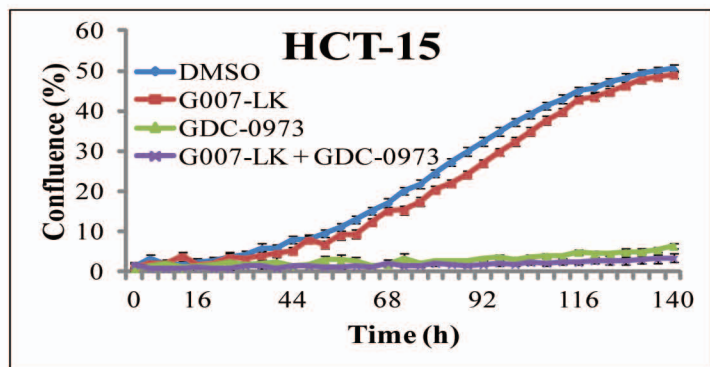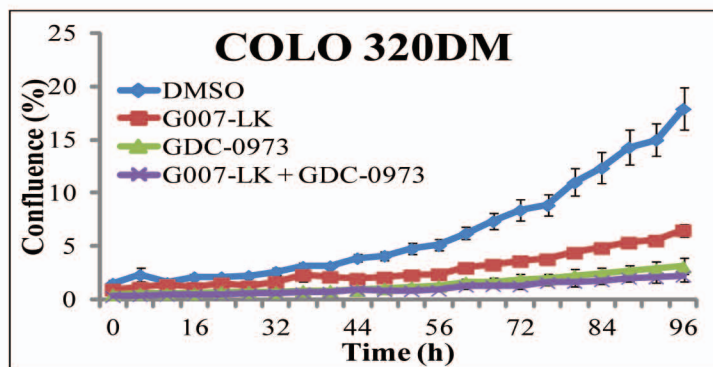
B) Western blot
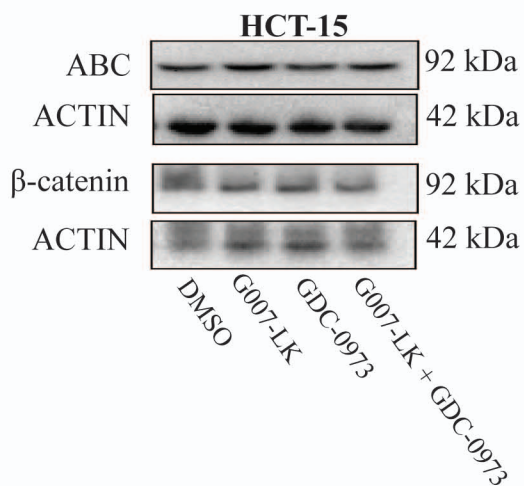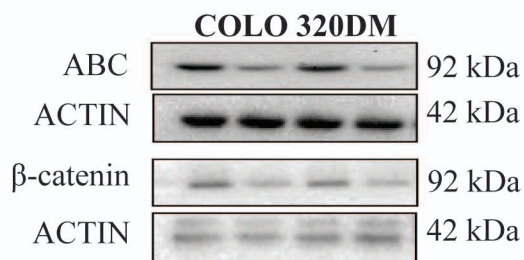
C) Immunofluorescence TNKS1/2 β-catenin merge
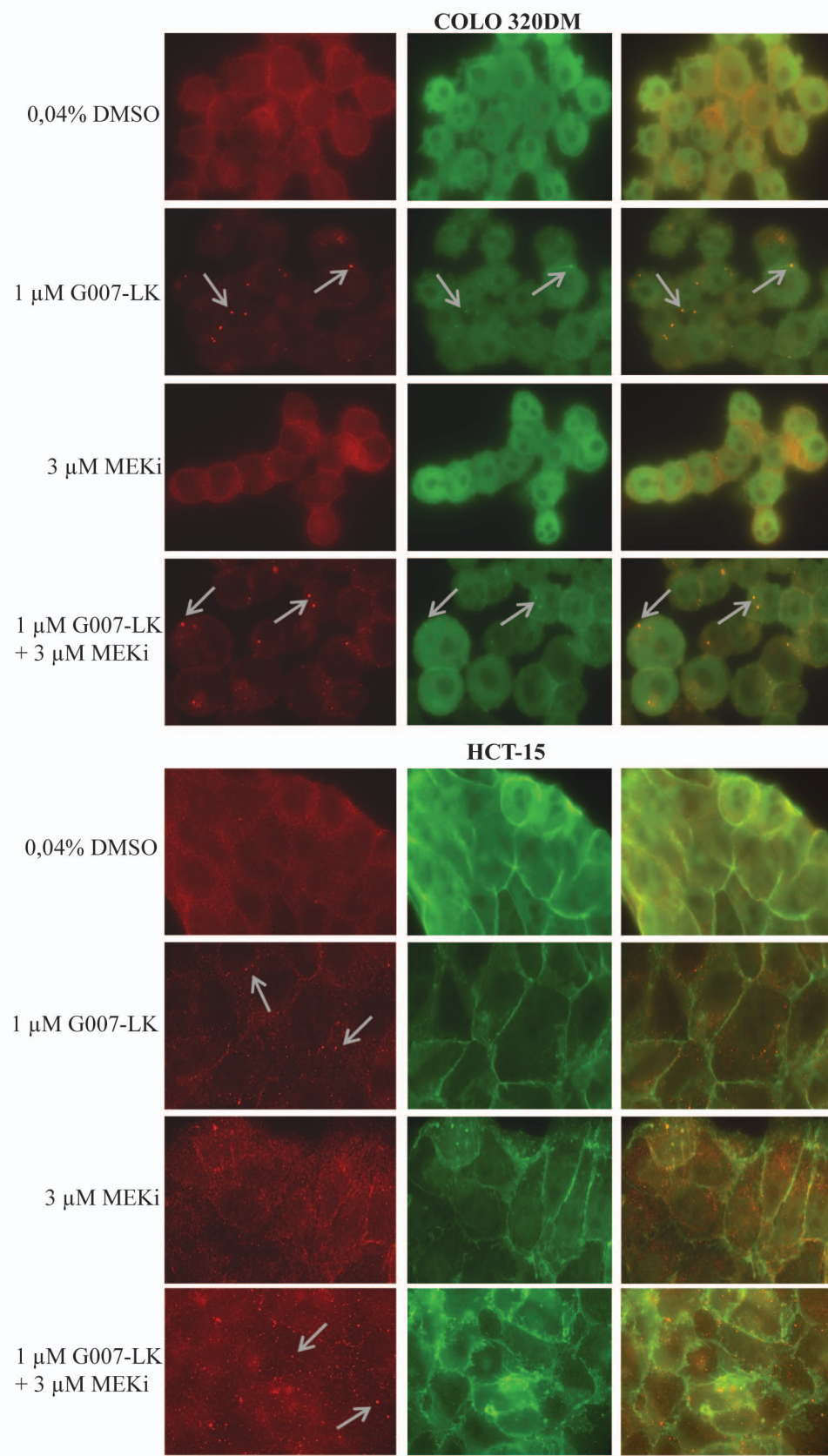
D) RT-qPCR
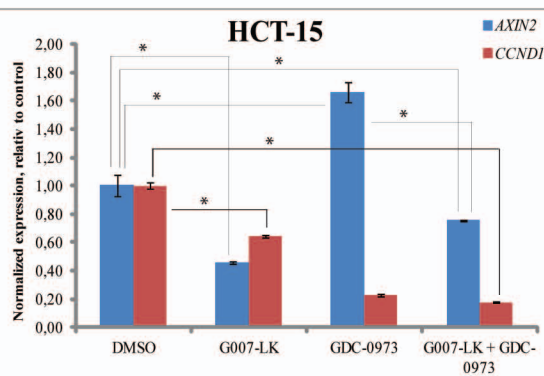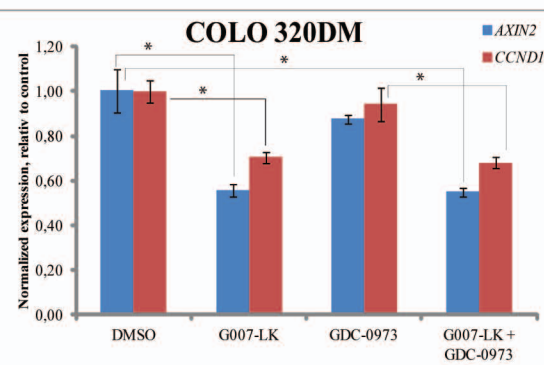
Figure 12. MEKi does not induce co-localization of TNKS1/2 and β-catenin in HCT-15 cells. A) Proliferation assay describing the change in sensitivity towards G007-LK treatment when combined with GDC-0973 from IncuCyte. COLO 320DM and HCT-15 cells treated with 0,04% DMSO (blue), 1 μM G007-LK (red), 3 μM GDC-0973 (green) and a combination of G007-LK and GDC-0973 (purple). B) Western blot protein analysis detecting levels of Non N-terminal phosphorylated (active) β-catenin (ABC) protein levels and total amount of β-catenin in both COLO 320DM and HCT-15 cells upon 0,04% DMSO, 1 μM G007-LK, 3 μM GDC-0973 and 1μM G007-LK + 3μM GDC-0973 treatment. C) Representative laser Whitefield microscopy pictures showing COLO 320DM and HCT-15 cells treated with 0,04% DMSO, 1 μM G007-LK, 3 μM GDC-0973, and G007-LK+GDC-0973 for 24 hours. The cells were further stained with Tankyrase-1/2 (H-350) rabbit for TNKS1/2 (red) and Purified Mouse Anti-β-catenin (green). D) Real time quantitative PCR analysis detecting levels of *AXIN2* and *CCND1* mRNA transcript in both COLO 320DM and HCT-15 cells treated with 0,04% DMSO, 1 μM G007-LK, 3 μM GDC-0973 and 1μM G007-LK + 3 μM GDC-0973.Statistics by Student`s t-test, 2 tailed, unequal variance, * = $p < 0,05$.

Inhibition of MEK does not induce co-localization between TNKS1/2 and β-catenin in HCT-15 cells

CRC cells show various degrees of sensitivity to TNKSi [50]. Recently, it was also observed that MEK is required for the recruitment of the β-catenin destruction complex to the cell membrane in *Drosophila*, upon WNT activation [20]. Upstream for MEK is RAS, where HCT-15 has a *KRAS* mutant background, while COLO 320DM has a *KRAS* wild type locus. The *KRAS* mutation is an activating mutation, leading to high amount of RAS in the cells. Interestingly, Schoumacher and collueagues claim to have found a strong synergy between TNKSi and MEKi which created a greater decrease in apoptosis in KRAS-mutated cancer cells [53]. We therefore asked whether the KRAS mutation in HCT-15 cells subsequently leads to insensitivity towards G007-LK, and whether MEK inhibition changes the sensitivity towards G007-LK in HCT-15 cells.

In COLO 320DM both TNKSi and 3 μM GDC-0973 (MEK inhibition; MEKi) treatment reduced proliferation as measured by IncuCyte live cell imaging system (figure 12a). A combination of both pathway inhibitors further reduced proliferation. In contrast, in HCT-15 cells TNKSi alone did not reduce proliferation, while MEKi led to a strong reduction in proliferation that was further diminished by combining TNKSi with MEKi.

TNKSi stabilizes the structural protein AXIN1/2, which are key structural proteins of the WNT/β-catenin destruction complex, in both COLO 320DM and HCT-15 cells [50], and are required for guiding the N-terminal phosphorylation of β-catenin as a step towards ubiquitination and proteasomal degradation. However, stabilization of AXIN1/2 does not necessarily imply β-catenin degradation (as shown in HCT-15 cells). We therefore analyzed whether the observed reduction in proliferation when using TNKSi and MEKi could be linked to altered β-catenin protein levels (figure 12b). In COLO 320DM cells, TNKSi reduced cellular levels of ABC as measured by Western blot protein analysis, while MEKi did not affect ABC levels. Hence, the increased effect of combining both pathway inhibitors may not be linked to altered β-catenin stability, but rather the inhibition of MEK and the EGFR-pathway. In HCT-15 cells, neither treatment reduced the protein levels of ABC.

In COLO 320DM cells, immunofluorescent staining revealed that MEKi had no affect on β-catenin subcellular distribution, indicating again that MEKi exerts its effects on proliferation in COLO 320DM through a mechanism that is independent of β-catenin (figure 12c). Interestingly, in HCT-15 cells MEKi changed β-catenin distribution, leading to a distinct cytoplasmic fraction of β-catenin. The combination of TNKSi and MEKi led to TNKSi induced TNKS1/2 clusters in the cytoplasmic membrane and in the cytoplasm, and MEKi induced release of β-catenin from the membrane, but still no co-localization of the two proteins at the detection level of immunofluorescence.

To further test the consequence of TNKSi alone and in combination with MEKi, RNA levels of the WNT/β-catenin target genes *AXIN2* and *CCND1* were measured (figure 12d). In COLO 320DM cells, TNKSi reduced both *AXIN2* and *CCND1* levels which correlates with the reduction of ABC protein levels and reduced proliferation. MEKi did not reduce *AXIN2* or *CCND1* levels, which is in agreement with the unaffected ABC protein levels in this cell line, but do not correspond to the reduced proliferation. In HCT-15 cells, TNKSi reduced both *AXIN2* and *CCND1* levels, although proliferation remained unaffected. In contrast, MEKi increased *AXIN2* levels, but strongly reduced *CCND1* transcript in accordance to both the release of β-catenin from the membrane to the cytoplasm, and the reduced proliferation rate. The

combination of TNKSi and MEKi normalized *AXIN2* transcript levels but further reduced *CCND1* transcript according to further reduction in proliferation.

Proliferation

A) COLO 320DM cells / HCT-15 cells
- EGFP esiRNA
- AXIN1 esiRNA
- AXIN 2 esiRNA
- AXIN1+2 esiRNA

B) TNKSi
- EGFP KD + DMSO
- EGFP KD + G007-LK
- AXIN1 KD + G007-LK
- AXIN2 KD + G007-LK
- AXIN 1+2 KD + G007-LK

C) MEKi
- EGFP KD + DMSO
- EGFP KD + GDC-0973
- AXIN1 KD + GDC-0973
- AXIN 2 KD + GDC-0973
- AXIN 1+2 KD + GDC-0973

D) TNKSi + MEKi
- EGFP KD + DMSO
- EGFP KD + G007-LK+GDC-0973
- AXIN 1 KD + G007-LK+GDC-0973
- AXIN 2 KD + G007-LK+GDC-0973
- AXIN 1+2 KD + G007-LK+GDC-0973

E) Western blot

AXIN 1 knock down | AXIN 1 + 2 knock down | AXIN 2 knock down

AXIN1
AXIN2
ACTIN

COLO 320DM + EGFP KD / COLO 320DM + AXIN1 KD / HCT-15 + EGFP KD / HCT-15 + AXIN1 KD
COLO 320DM + EGFP KD / COLO 320DM + AXIN1+2 KD / HCT-15 + EGFP KD / HCT-15 + AXIN1+2 KD
COLO 320DM + EGFP KD / COLO 320DM + AXIN2 KD / HCT-15 + EGFP KD / HCT-15 + AXIN2 KD

Figure 8. Significant changes in proliferation upon AXIN knock down in COLO 320DM and HCT-15 cells. Proliferation rate measured in IncuCyte with COLO 320DM and HCT-15 cells transfected with EGFP esiRNA (blue), AXIN1 esiRNA (red), AXIN 2 esiRNA (green) and a combination of both AXIN1 and AXIN2 esiRNA (purple). A) untreated cells. B) Cells treated with TSNKi. C) Cells treated with MEKi. D) Cells treated with TNKS combined with MEKi. E) Western blot protein analysis validating the esiRNA mediated KD effect.

Significant changes in proliferation upon AXIN knock down in COLO 320DM and HCT-15 cells

Further we wanted to analyze whether the MEKi decreased proliferation in both COLO 320DM and HCT-15 cells may be due to any regulation of AXIN1/2. We analyzed the involvement of AXIN1/2 with both single and combined AXIN1 and AXIN2 KD.

In COLO 320DM cells, both AXIN1 and AXIN2 KD increased proliferation rate figure 13a). This result correspond with previous research about AXIN1/2 scaffolding the WNT/β-catenin destruction complex, enabling the complex to bind and phosphorylate β-catenin and label the protein for subsequent proteosomal degradation. However, protein analysis of ABC was not performed in this assay due to time issues. HCT-15 cells treated with esiRNA revealed an increased proliferation when both AXIN1 and AXIN2 were knocked down; indicating that AXIN1/2 are negative factors of proliferation in this cell line. However, this proliferative regulation cannot be through down-regulation of β-catenin, as the cell line is proved to have β-catenin independent growth.

Upon TNKSi, cells treated with EGFP esiRNA showed reduced proliferation in COLO 320DM cells (figure 13b). However, when knocking down AXIN1 and AXIN2, this counteracted an increased proliferation rate, which validated the TNKSi effect on this cell line. The TNKSi treatment works by stabilizing AXIN1/2 in the cytoplasm, so the WNT/β-catenin destruction complex can rearrange and be active again, thus G007-LK mediated reduction in proliferation is AXIN1/2 dependent. Interestingly, HCT-15 cells became sensitive to TNKSi upon AXIN1/2 KD, which would mean that the TNKSi insensitivity is due to AXIN1/2 itself.

When treated both COLO 320DM and HCT-15 cells with AXIN1/2 KD and MEKi, there was observed increased levels of proliferation in AXIN2 KD cells, but oppositely reduced proliferation in AXIN1 KD cells, compared to the EGFP + MEKi sample (figure 13c). For the TNKSi the dependency on AXIN1/2 was well known, however, how MEKi affect the proliferation in this cell line is not fully understood. However, these results indicate that MEKi may be affecting the cell lines through AXIN1.

The western blot analysis revealed a mild reduction of AXIN1 and AXIN2 upon AXIN1/2 KD in both cell lines. However, there is strong indication of change in the cells upon proliferation rates. This experiment was only done ones due to time issues, and should be repeated.

5. Discussion

As shown in figure 13, knock down of AXIN1 and AXIN2 created some very interesting results, quite opposite between the COLO 320DM and HCT-15 cell lines. Analyzed against the control sample revealed the most diverging results in COLO 320DM cells were due to AXIN2 knock down, while the most deviant results in the HCT-15 cell line were due to AXIN1 knock down.

Chia and Costantini claim that the two related proteins AXIN1 and AXIN2 are thought to perform similar functions and the explanation for the lack of redundancy between the two proteins are due to their different expression mode [54]. Interestingly, Thorvaldsen and colleagues found that the SW480 colorectal cell line was entirely dependent on AXIN2 to succeed formation of WNT/β-catenin destruction complexes and degradation of β-catenin, while AXIN1 was not required [49]. However, recruitment of AXIN1/2 and the WNT/β-catenin destruction complex to the cell membrane, upon WNT ligand binding, primarily involves the recruitment of AXIN1 [55]. Our results confirms the theories postulated by Thorvaldsen [49] and Bernkopfˋs [55] that the cells have two different destruction complexes (further referred to signalosome and degradasome), where AXIN1 is the main AXIN protein in the signalosome complex, and AXIN2 is the main AXIN protein in the degradasome complex. The degradasome is localized in the cytoplasm while the signalosome is located in the membrane. Both AXIN1/2 are postulated to be present in both complexes, and are able to partially compensate for the main AXIN protein, if necessary.
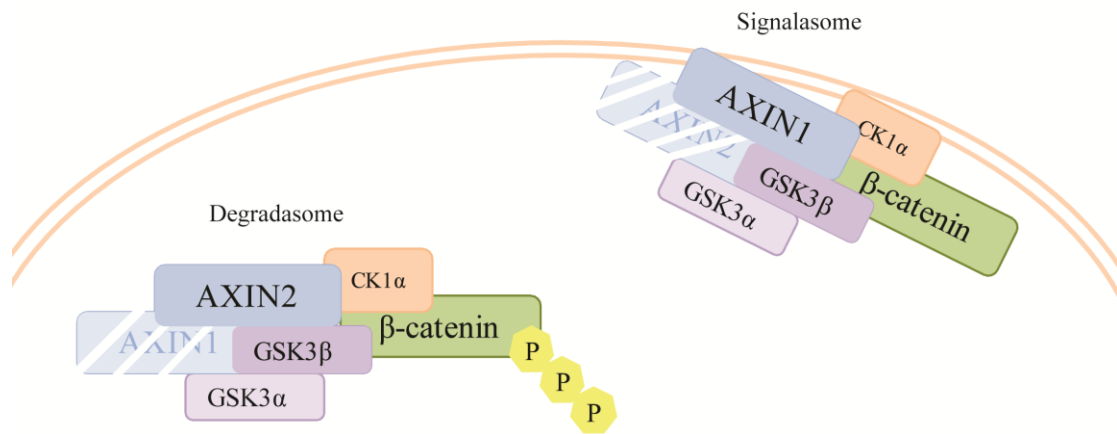
Figure 14. Simplified, schematic drawing of the degradasome and signalosome. Degradasomes are located in the cytoplasm where AXIN2 is the main AXIN protein, and where β-catenin is phosphorylated and targeted for degradation. The signalosome is located in the cell membrane, where AXIN1 is the main AXIN protein. The signalosome activates the WNT/β-catenin signaling pathway inside the cell upon WNT ligand binding, by preventing β-catenin degradation.

AXIN2 is co-localized with TNKS1/2 in both COLO 320DM and HCT-15 cells upon TNKSi, as shown in figure 6. However, we believe that AXIN1 is also co-localized with both AXIN2 and TNKS1/2 in both COLO 320DM and HCT-15 cells. To validate this, an immunofluorescent assay with AXIN1 would be essential. However, the strong decrease in proliferation upon AXIN1 knock down in HCT-15 cells indicates importance of this protein.

In addition to both AXIN1/2 we believe that the two WTN/β-catenin complexes also contain both GSK3α and GSK3β. In figure 9a, the immunofluorescence analysis showed that GSK3α was co-localized with TNKS1/2 upon G007-LK treatment in the COLO 320DM control sample (EGFP knock down). However, there is believed that GSK3β is the main protein to phosphorylate cytoplasmic β-catenin. We were not able to detect any co-localized clusters between TNKS1/2 and GSK3α in control HCT-15 cells or in cells with GSK3β knock down. To determine whether GSK3α is present in the WNT/β-catenin destruction complex in HCT-15 cells, a pull down assay of TNKS1/2 would be necessary to solidly claim its binding partners. To differ between the functional vs. structural role of GSK3α and GSK3β we could have repeated the assay with a GSK3 inhibitor, e.g. CHIR.

As previous mentioned the AXIN2 KD affected cell proliferation (increased) more than AXIN1 KD in the COLO 320DM cell line, confirming its role in the degradasomes to promote degradation of β-catenin. Oppositely, the signalosome is proposed as the main complex in the HCT-15 cell line, where β-catenin is not degraded. The determination mechanism of which main AXIN complex the cell lines mainly use is not fully understood. One possibility is the truncation of the *APC* gene, which is believed to decide the cell`s sensitivity towards tankyrase inhibition [56].

Kohler and colleagues claims the "CID" domain in the *APC* gene is located between the second and third 20 amino acid repeat domains (AARs), and is believed to contain β-catenin binding domain [57].
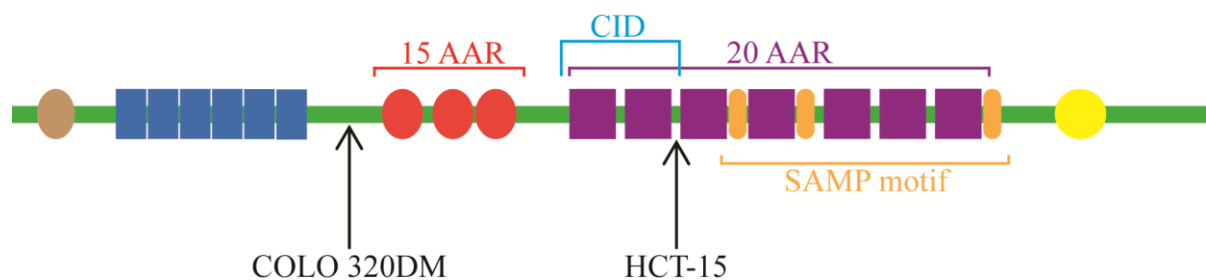
Figure 15. A schematic representation of truncating mutations in COLO 320DM and HCT-15 cell lines at the *APC* gene. Modified from figure 2 in Lau et.al [50] AAR; amino acid repeat domain, CID; catenin inhibitory domain, SAMP; ser-ala-met-pro.

The HCT-15 cell lines APC truncation at codon position 1417 is localized right after the CID domain, however right before the three AXIN-binding SAMP motifs. Due to this interesting knowledge, an assay was sat up to investigate whether the APC protein in HCT-15 cells holds β-catenin away from the β-catenin destruction complex, thus inhibiting the phosphorylation and subsequent degradation (appendix 1). The results revealed very poor quality on the APC knock down with esiRNA, which means the data is not trustable. Due to time issues, the assay was not repeated. However it would be interesting to do the assay again to find β-catenin`s location upon APC KD.

Additionally, Tanaka and colleagues claim that the long APC mutant (retaining two or more 20 AARs) exerts a dominant negative effect on AXIN-dependent β-catenin degradation upon TNKSi [56]. Thus, analyze of ABC protein levels upon APC KD with TNKSi would be interesting, to see if the APC mutation in HCT-15 cells is responsible for the sensitivity level towards tankyrase inhibition.

In the HCT-15 cell line upon TNKSi, complexes containing TNKS1/2, GSK3β and AXIN2 were observed at the cell membrane, with immunofluorescent analysis (figure 6). However, to validate the actual binding between the complexes and the membrane receptors, analysis of TNKS1/2`s binding partners, trough a pull-down assay would be an option. Mainly look for LRP5/6, since LRP5/6 is proposed to inhibit the WNT/β-catenin destruction complex upon WNT signaling, by phosphorylating AXIN [58]. For now, the immunofluorescent results indicate that the WNT/β-catenin destruction complexes could possibly be bound to the membrane receptors in HCT-15 cells, which validates our theory together with Hall and Verheyens article [20].

Interestingly, Hall and Verheyens claim that upon WNT ligand binding to the membrane receptors in *Drosophila* development, MEK is required for the recruitment of the β-catenin destruction complex to the membrane. As previous mentioned the HCT-15 cell line has a *KRAS* mutation located upstream for MEK. The mutation leads to an accumulation of RAS proteins, and the thought was that MEK may have the same binding effect on the WNT/β-catenin destruction complex in human cells as in *Drosophila*. Excitingly, in the HCT-15 cell line, the combination of both MEKi and TNKSi created a release of membrane occupied TNKS1/2 clusters, which could indicate that MEK is recruiting the WNT/β-catenin destruction complex to the membrane also in human cells (figure 12c). However, TNKS1/2 and β-catenin was not co-localized in the TNKS1/2 clusters, and the treatment combination did not lead to any reduction in ABC. One possible option may be that the HCT-15 CRC cell line has adapted which consequently decrease the importance of the WNT/β-catenin signaling pathway considering proliferation and survival. In this way, the importance of AXIN1 and the signalosome could be increased due to signaling through another pathway, which also explains the β-catenin independent proliferation and survival.

KRAS wild type COLO 320DM cells does not contain TNKS1/2 clusters by the membrane. Instead, the COLO 320DM cell line had TNKS1/2 clusters in the cytoplasm, which were co-localized with β-catenin upon TNKSi. These cytoplasmic clusters even further validate the new theory, claiming that the degradasomes are the main AXIN complex in COLO 320DM, and that these cytoplasmic clusters cause degradation of active β-catenin, with subsequent reduction of WNT signaling, upon TNKSi.

When analyzing the cell proliferation in both COLO 320DM and HCT-15 cells, some very interesting results occurred. In normal COLO 320DM cells, the regular exponential proliferation is crucially decreased upon TNKSi as viewed in figure 7b. This is expected by the stabilization of the degradasomes in the cytoplasm. However, when inhibiting the WNT/β-catenin destruction complex by knocking out GSK3β with DMSO control treatment, a tremendous decrease in proliferation occur (figure 8c), even though ABC protein levels and *AXIN2* transcript levels increases. This result indicate that the proliferation in COLO 320DM cells must be overly affected by another pathway were GSK3β have a crucial role. In the HCT-15 cell line, TNKSi alone did not affect either proliferation or protein levels of ABC measured against the control (figure 7b). Despite this, a clear decrease in both *AXIN2* and *CCND1* transcript levels occur, validated by the same decrease in *STF luciferase* activity. However, this phenomenon is not fully understood, but has to be regulated by another mechanism than through the WNT/β-catenin signaling pathway.

Interestingly, when transfecting the HCT-15 cells with GSK3β esiRNA, the protein levels of ABC decreased (figure 8b). ABC protein levels of the EGFP transfected HCT-15 cells with TNKSi were not at all affected. Even with this extreme difference between the EGFP KD + TNKSi and GSK3β KD + TNKSi, the exact same decrease occurred in *AXIN2* mRNA transcript levels. This validates that GSK3β is regulating the HCT-15 cell line through another mechanism.

When investigating the proliferation, the results showed no regulation in TNKSi sensitivity neither with nor without GSK3β knock down in HCT-15 cells. However, in HCT-15 cells with GSK3β KD, a massive decrease in proliferation occurred, independent on the TNKSi treatment. This result indicates that the proliferation in

HCT-15 cells is independent on the WNT/β-catenin signaling pathway. The theory about a WNT/β-catenin pathway independent proliferation was further validated upon the β-catenin KD assay (figure 11), where neither the proliferation nor the sensitivity towards TNKSi was affected by the removal of β-catenin in the HCT-15 cell line. However, in COLO 320DM, the proliferation is affected with decreased proliferation upon GSK3β KD, even though the cell line was found to have a β-catenin dependent proliferation. Even though levels of ABC increased with GSK3β KD + DMSO treatment, the proliferation is massively reduced, indicating involvement of a second pathway.

Similarly, there is believed that the massive decreases in proliferation upon MEKi in HCT-15 cells are due to regulations through another pathway than the WNT/β-catenin signaling pathway, most likely through the EGFR-pathway. MEKi created a decrease in *CCND1* mRNA transcript levels, and opposite a strong increase in *AXIN2* levels. However, protein levels of ABC was not regulated upon MEKi in HCT-15 cells, which was further validated with no regulation discovered in the total amount of β-catenin protein levels in the cells (figure 12). This further underpins that there may be some regulations of AXIN1 or GSK3β protein levels that creates the proliferation drop upon MEK inhibition, in HCT-15 CRC cells.

6. Conclusion

We believe that degradasomes, with regard to β-catenin degradation, is not important in the tankyrase inhibitor insensitive colorectal cancer cell line HCT-15. In the HCT-15 cells, β-catenin is not under any tested conditions co-localized with the degradasomes upon TNKSi. Furthermore, knock down of GSK3β leads to both down regulation of ABC and reduced proliferation. The decrease in proliferation is not due to regulated β-catenin, since β-catenin mediated knock down does not change proliferation in HCT-15 cells.

We observed that AXIN proteins restrains proliferation of both COLO 320DM and HCT-15 colorectal cancer cell lines. We also observed that removal of AXIN proteins potentiates HCT-15 cells for TNKSi.

7. List of literature

1. Folkehelseinstituttet, *Snart er det kreft som tar flest liv*. Folkehelseinstituttet: www.fhi.no.
2. Folkehelseinstituttet, *Fakta om kreft - forekomst og dødelighet* Folkehelseinstituttet.
3. registeret, K., *Kreftstatistikk* KREFT registeret.
4. registeret, K., *Nasjonalt kvalitetsregister for tykk- og endetarmskreft* KREFT registeret: www.kreftregisteret.no.
5. Cooper, G.M. and R.E. Hausman, *The cell*. 2000: Sinauer Associates Sunderland.
6. Sameer, A.S.S., *Colorectal cancer: molecular mutations and polymorphisms.* Frontiers in oncology, 2013. **3**: p. 114.
7. Norge, H. *Tykk- og endetarmskreft (tarmkreft)*. 16.06.2016 11.01.17]; Available from: https://helsenorge.no/sykdom/kreft/tarmkreft.
8. Chung, D.C., *The genetic basis of colorectal cancer: insights into critical pathways of tumorigenesis.* Gastroenterology, 2000. **119**(3): p. 854-865.
9. Vasen, H., et al., *Decision analysis in the management of duodenal adenomatosis in familial adenomatous polyposis.* Gut, 1997. **40**(6): p. 716-719.
10. Smith, G., et al., *Mutations in APC, Kirsten-ras, and p53—alternative genetic pathways to colorectal cancer.* Proceedings of the National Academy of Sciences, 2002. **99**(14): p. 9433-9438.
11. McMichael, A.J. and G.G. Giles, *Cancer in migrants to Australia: extending the descriptive epidemiological data.* Cancer Research, 1988. **48**(3): p. 751-756.
12. Zhai, Y., et al., *Role of β-catenin/T-cell factor-regulated genes in ovarian endometrioid adenocarcinomas.* The American journal of pathology, 2002. **160**(4): p. 1229-1238.
13. Lustig, B. and J. Behrens, *The Wnt signaling pathway and its role in tumor development.* Journal of cancer research and clinical oncology, 2003. **129**(4): p. 199-221.
14. Brocardo, M. and B.R. Henderson, *Detection of cytoplasmic and nuclear localization of adenomatous polyposis coli (APC) protein in cells.* Wnt Signaling: Pathway Methods and Mammalian Models, 2008: p. 77-89.
15. Conlin, A., et al., *The prognostic significance of K-ras, p53, and APC mutations in colorectal carcinoma.* Gut, 2005. **54**(9): p. 1283-1286.
16. Albuquerque, C., et al., *Colorectal cancers show distinct mutation spectra in members of the canonical WNT signaling pathway according to their anatomical location and type of genetic instability.* Genes, Chromosomes and Cancer, 2010. **49**(8): p. 746-759.
17. Schubbert, S., K. Shannon, and G. Bollag, *Hyperactive Ras in developmental disorders and cancer.* Nature Reviews Cancer, 2007. **7**(4): p. 295-308.
18. Minamoto, T., M. Mai, and Z.e. Ronai, *K-ras mutation: early detection in molecular diagnosis and risk assessment of colorectal, pancreas, and lung cancers--a review.* Cancer detection and prevention, 1999. **24**(1): p. 1-12.
19. Bos, J.L., *Ras oncogenes in human cancer: a review.* Cancer research, 1989. **49**(17): p. 4682-4689.
20. Hall, E.T. and E.M. Verheyen, *Ras-activated Dsor1 promotes Wnt signaling in Drosophila development.* J Cell Sci, 2015. **128**(24): p. 4499-4511.
21. Steele, R., et al., *The p53 tumour suppressor gene.* British Journal of Surgery, 1998. **85**(11): p. 1460-1467.
22. Hollstein, M., et al., *p53 mutations in human cancers.* Science, 1991. **253**(5015): p. 49-54.
23. Barker, N., *The canonical Wnt/β-catenin signalling pathway.* Wnt Signaling: Pathway Methods and Mammalian Models, 2008: p. 5-15.
24. Alman, B.A., et al., *Increased beta-catenin protein and somatic APC mutations in sporadic aggressive fibromatoses (desmoid tumors).* The American journal of pathology, 1997. **151**(2): p. 329.
25. Salahshor, S. and J. Woodgett, *The links between axin and carcinogenesis.* Journal of clinical pathology, 2005. **58**(3): p. 225-236.
26. Logan, C.Y. and R. Nusse, *The Wnt signaling pathway in development and disease.* Annu. Rev. Cell Dev. Biol., 2004. **20**: p. 781-810.
27. Jaiswal, A.S., et al., *[beta]-Catenin-mediated transactivation and cell-cell adhesion pathways are important in curcumin (diferuylmethane)-induced growth arrest and apoptosis in colon cancer cells.* Oncogene, 2002. **21**(55): p. 8414.
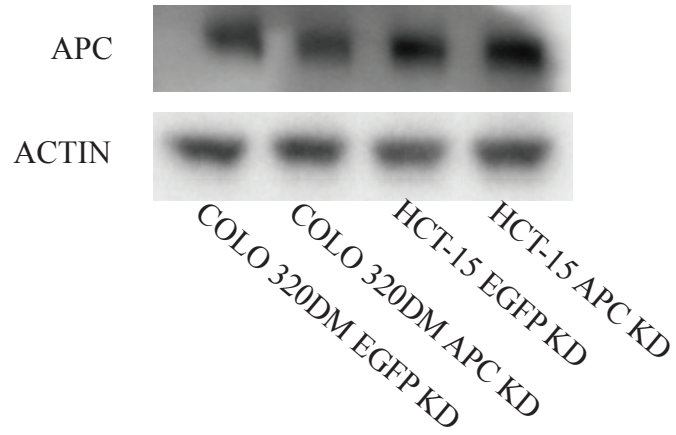
28.   Suzuki, H., et al., *Epigenetic inactivation of SFRP genes allows constitutive WNT signaling in colorectal cancer.* Nature genetics, 2004. **36**(4): p. 417-422.

29.   Huang, S.-M.A., et al., *Tankyrase inhibition stabilizes axin and antagonizes Wnt signalling.* Nature, 2009. **461**(7264): p. 614-620.

30.   Voronkov, A., et al., *Structural basis and SAR for G007-LK, a lead stage 1, 2, 4-triazole based specific tankyrase 1/2 inhibitor.* Journal of medicinal chemistry, 2013. **56**(7): p. 3012-3023.

31.   De Rycker, M. and C.M. Price, *Tankyrase polymerization is controlled by its sterile alpha motif and poly (ADP-ribose) polymerase domains.* Molecular and cellular biology, 2004. **24**(22): p. 9802-9812.

32.   Smith, S., et al., *Tankyrase, a poly (ADP-ribose) polymerase at human telomeres.* Science, 1998. **282**(5393): p. 1484-1487.

33.   Zhang, Y., et al., *RNF146 is a poly (ADP-ribose)-directed E3 ligase that regulates axin degradation and Wnt signalling.* Nature cell biology, 2011. **13**(5): p. 623-629.

34.   Tian, X.-H., et al., *XAV939, a tankyrase 1 inhibitior, promotes cell apoptosis in neuroblastoma cell lines by inhibiting Wnt/β-catenin signaling pathway.* Journal of Experimental & Clinical Cancer Research, 2013. **32**(1): p. 1.

35.   Tian, X.-H., et al., *XAV939, a tankyrase 1 inhibitior, promotes cell apoptosis in neuroblastoma cell lines by inhibiting Wnt/β-catenin signaling pathway.* Journal of Experimental & Clinical Cancer Research, 2013. **32**(1): p. 100.

36.   Waaler, J., et al., *A novel tankyrase inhibitor decreases canonical Wnt signaling in colon carcinoma cells and reduces tumor growth in conditional APC mutant mice.* Cancer research, 2012. **72**(11): p. 2822-2832.

37.   Waaler, J., et al., *Novel synthetic antagonists of canonical Wnt signaling inhibit colorectal cancer cell growth.* Cancer Research, 2011. **71**(1): p. 197-205.

38.   ATCC, *COLO 320DM (ATCC CCL-220).*

39.   ATCC, *HCT-15 (ATCC CCL-225).* ATCC.

40.   Nikfarjam, L. and P. Farzaneh, *Prevention and detection of Mycoplasma contamination in cell culture.* Cell j (Yakhteh), 2011. **13**(4).

41.   BioResearch, L., *MycoAlert™ Mycoplasma Detection Kit*.

42.   SIGMA-ALDRICH. *RT-PCR and RT-qPCR.* 03.05.17]; Available from: http://www.sigmaaldrich.com/life-science/molecular-biology/molecular-biology-products.html?TablePage=9620584.

43.   Promega, *Technical manual Dual-Luciferase Reporter 1000 Assay System, Instruction for use of Product E1980.* 2009, Promega.

44.   Ungar, A.R., K.A. Helde, and R.T. Moon, *Production of androgenetic haploids in zebrafish with ultraviolet light.* Molecular marine biology and biotechnology, 1998. **7**: p. 320-326.

45.   Theis, M. and F. Buchholz, *MISSION esiRNA for RNAi screening in mammalian cells.* JoVE (Journal of Visualized Experiments), 2010(39): p. e2008-e2008.

46.   Mahmood, T. and P.-C. Yang, *Western blot: technique, theory, and trouble shooting.* North American journal of medical sciences, 2012. **4**(9): p. 429.

47.   BioRad, *ChemiDoc™ Touch Imaging System*.

48.   Maity, B., D. Sheff, and R.A. Fisher, *Immunostaining: detection of signaling protein location in tissues, cells and subcellular compartments.* Methods in cell biology, 2012. **113**: p. 81-105.

49.   Thorvaldsen, T.E., et al., *Differential Roles of AXIN1 and AXIN2 in Tankyrase Inhibitor-Induced Formation of Degradasomes and β-Catenin Degradation.* PloS one, 2017. **12**(1): p. e0170508.

50.   Lau, T., et al., *A novel tankyrase small-molecule inhibitor suppresses APC mutation–driven colorectal tumor growth.* Cancer research, 2013. **73**(10): p. 3132-3144.

51.   Thorvaldsen, T.E., et al., *Structure, dynamics, and functionality of tankyrase inhibitor-induced degradasomes.* Molecular Cancer Research, 2015. **13**(11): p. 1487-1501.

52.   Doble, B.W., et al., *Functional redundancy of GSK-3α and GSK-3β in Wnt/β-catenin signaling shown by using an allelic series of embryonic stem cell lines.* Developmental cell, 2007. **12**(6): p. 957-971.

53.   Schoumacher, M., et al., *Inhibiting Tankyrases sensitizes KRAS-mutant cancer cells to MEK inhibitors via FGFR2 feedback signaling.* Cancer research, 2014. **74**(12): p. 3294-3305.

54.   Chia, I.V. and F. Costantini, *Mouse axin and axin2/conductin proteins are functionally equivalent in vivo.* Molecular and cellular biology, 2005. **25**(11): p. 4371-4376.

55. Bernkopf, D.B., M.V. Hadjihannas, and J. Behrens, *Negative-feedback regulation of the Wnt pathway by conductin/axin2 involves insensitivity to upstream signalling.* J Cell Sci, 2015. **128**(1): p. 33-39.

56. Tanaka, N., et al., *APC mutations as a potential biomarker for sensitivity to tankyrase inhibitors in colorectal cancer.* Molecular Cancer Therapeutics, 2017: p. molcanther.0578.2016.

57. Kohler, E.M., et al., *β-Catenin degradation mediated by the CID domain of APC provides a model for the selection of APC mutations in colorectal, desmoid and duodenal tumours.* Human molecular genetics, 2009. **18**(2): p. 213-226.

58. Mi, K. and G.V. Johnson, *Role of the intracellular domains of LRP5 and LRP6 in activating the Wnt canonical pathway.* Journal of cellular biochemistry, 2005. **95**(2): p. 328-338.

Appendix 1. APC KD results

Appendix figure 1. APC knock down. A) Western blot protein analysis revealing poor quality on APC esiRNA mediated KD. B) HCT-15 cells transfected with EGFP esiRNA (control) and APC esiRNA, and treated with 0,04 % DMSO, 1 µM TNKSi and a combination of TNKSI and MEKi. The cells were further immunofluorescent stained with antibodies detecting TNKS1/2 (red) and β-catenin (green).

A) Western blot

APC

ACTIN

COLO 320DM EGFP KD
COLO 320DM APC KD
HCT-15 EGFP KD
HCT-15 APC KD

B) Immunofluorescence with APC knock down

HCT-15

TNKS

β-catenin

Merge

EGFP KD
DMSO

EGFP KD
G007-LK

EGFP KD
G007-LK
+
GDC-0973

APC KD
DMSO

APC KD
G007-LK

APC KD
G007-LK
+
GDC-0973
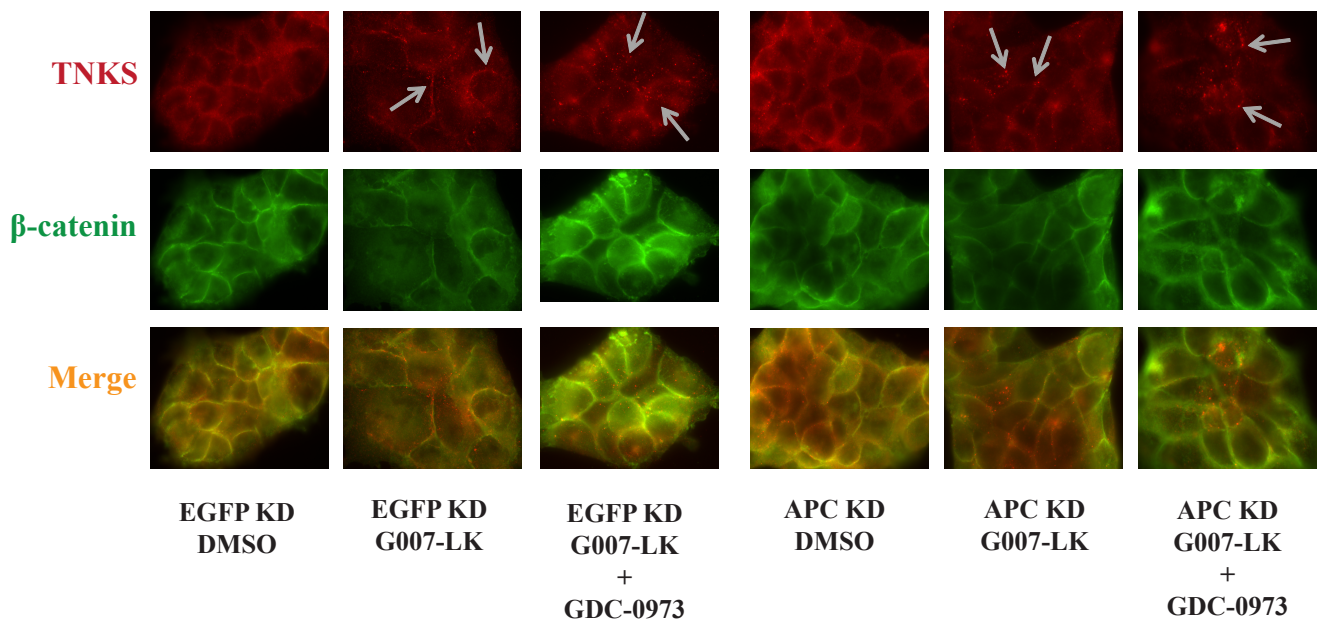
Appendix 2. Abbreviations

ABC	Non N-terminal phosphorylated (active) b-catenin
APC	Adenomatous polyposis coli
ATCC	American Type Culture Collection
AXIN1	Axis inhibition protein 1
AXIN2	Axis inhibition protein 2
cDNA	Complementary deoxyribonucleic acid
CK1α	Casein kinases 1α
CRC	Colorectal cancer
DAPI	4', 6-diamidino-2-phenylindole
DMSO	Dimethyl sulfoxide
DVL	Disheveled
EDTA	Ethylenediaminetetraacetic acid
EGFR	Epidermal growth factor receptor
ERK	Extracellular signal-regulated kinase
FBS	Fetal bovine serum
FZD	Frizzled
GAPDH	Glyceraldehyde-3-phosphate dehydrogenase
GDP	Guanosine diphosphate
GSK3β	Glycogen synthase kinase 3β
GTP	Guanosine triphosphate
HRP	Horseradish peroxidase
KD	Knock down
LEF	Lymphoid enhancer factor
LRP5/6	Lipoprotein receptor-related protein 5/6
MAPK	Mitogen-activated protein kinase
MEK	Mitogen-activated protein kinase kinase
mRNA	Messenger ribonucleic acid
P-ERK	Phosphorylated extracellular signal-regulated kinase
P	Passage
PARP	Poly (ADP-ribose) polymerase
PBS	Phosphate-buffer saline

PI3K	Phosphatidylinositide 3-kinase
PVDF	Polyvinyliden fluoride
RAF	Rapidly accelerated fibrosarcoma
RAS	Rat sarcoma
RNF146	Ring finger protein
RT-qPCR	Real-time quantitative polymerase chain recation
SAM	Sterile alpha motif
TCF	T-cell factor
TGF-β	Transforming growth factor beta
TNKS	Tankyrase
WNT	Wingless-type mammary tumor virus integration site proteins
β-TRCP	Beta-transducin-repeatcontaining protein

Appendix 3. Complete material list

Material	Producer	Catalog nr.
Cell culturing		
COLO 320DM	ATCC (LGC-standards)	CCL-220
HCT-15	ATCC (LGC standards)	CCL-225
RPMI-1640 Medium	Sigma Aldrich	R8758
Fetal bovine serum (FBS), ES qualified	Life Technologies	16141-079
Penicillin-streptomycin	Sigma Aldrich	P4333
Trypsin – Ethylenediaminetetraacetic acid (EDTA)	Sigma Aldrich	T3924
1X PBS	Ullevål universitetssykehus, mikrobiologisk avdeling	-
MycoAlert Mycoplasma detection kit	Fischer	11680271
Cell treatments		
G007-LK	ChemRoyal Inc.	-
Dimethyl sulfoxide (DMSO)	Sigma Aldrich	D8418
GDC-0973	Med Chem express	HY-13064
Luciferase-assay		
FuGENE® HD Transfection Reagent	Promega	E2311
Opti-MEM	Invitrogen	31985-047
Super Top-Flash pTA-Luc vector	A gift from R. Moon	[44]
Renilla pRL-TK Vector	Promega	E2241
Dual-Luciferase Reporter Assay 1000 assay kit	Nerliens Meszansky	E1980
SDS-PAGE and Western blot		
Methanol	VWR	20903.368
Pierce® RIPA Buffer	Thermo Scientific	89901
cOmplete Tablets – Protease inhibitor Cocktail Tablets	Roche applied science	4693124001
PhosSTOP – Phosphatase Inhibitor Cocktail Tablets	Roche applied science	04906837001
Nu-PAGE® Tris-Acetate SDS running buffer 20X	Life Technologies	LA0041
Nu-PAGE® MOPS SDS running buffer 20X	Life Technologies	NP0001

Nu-PAGE® Novex® 3-8% Tris-Acetate Protein gels, 1.0 mm, 10 well	Life Technologies	NP0321BOX
Nu-PAGE® Novex® 4-12% Bis-Tris Protein gels, 1.0 mm 10 well	Life Technologies	EA0375BOX
PageRuler Prestained Protein Ladder	Thermo Fisher Scientific	26616
Immobilon® - P^{SQ} Transfer Membranes	Merck Life Science/ Millipore	ISEQ00010
Extra thick blot paper	Bio-Rad Laboratories	1703960
Nonfat dried milk	AppliChem	A0830,0500
Tris buffered saline (TBS) tablets	Medicago	09-7510-100
Kit ECL Prime Western Blotting Detection Reagent	GE Healthcare Amersham	RPN2236
Transfer buffer		
Trizma-base	Sigma Aldrich	T1503
Glycine	Sigma Aldrich	G7126
SDS loading buffer (5X)		
Tris hydrochloride	Sigma Aldrich	T-3253
Glycerol	Sigma	G5516-1L
Sodium dodecyl sulfate	Sigma	L3771-100G
Bromophenol blue	Sigma Aldrich	BO126-25G
2-mercaptoethanol	Sigma Aldrich	M6250
Immunofluorescence		
Presisjonsdekkglass, runde	VWR	MARI0117580
Microscope slides	Marienfeld	10 002 00
ProLong® Diamond Antifade Mountant	Life Technologies	P36965
Poly-lysin solution	Sigma Aldrich	P8920
Fluoroshield with DAPI	Sigma Aldrich	F6057
Triton X-100	Roche applied science	10 789 704 001
4% PFA		
Paraformaldehyde powder	Fisher	04042
Sodium hydroxide (NaOH)	VWR	1.06462.5000
4% BSA/PBS		
BSA Cohn fraction V, Proteasfri	SAVEEN WERNER AB	B2000-100
Transfection with esiRNA		
Opti-MEM	Invitrogen	31985-047
Lipofectamin 2000	Life Technologies (invitrogen)	11668-019

RT-qPCR		
GenElute Mammalian Total RNA Purification Kit	Sigma Aldrich	RTN350
SuperScript VILO cDNA synthesis Kit	Life Technologies	4369510
TaqMan Gene Expression Mastermix	Life Technologies	4309849